

Università degli Studi di Salerno

Facoltà di Scienze Matematiche,
Fisiche e Naturali



“Redox proteins for the development of biosensors”

Corso di Dottorato in Chimica IX Ciclo

Anno Accademico 2007 – 2010

Candidato
Franco De Martino

Franco De Martino

Tutor
Prof. Claudio Pellecchia

*A chi percorre la mia stessa strada...
perché la felicità non viene stando seduti ad
aspettarla.*

Chapter one - Introduction	1
Abstract	1
Optical Biosensors.....	2
The proteins used in this work as molecular recognition elements for toxic gases.....	4
Heme proteins	4
CcP (Cytochrome c peroxidase)	6
Mb (Myoglobin)	7
Fluorescence	8
F.R.E.T. (Forster resonance energy transfer).....	10
The analytes under investigation: NO and H ₂ S	12
Nitric oxide	12
An application of the labeled –CcP system as NO biosensor: an example <i>in vivo</i>	16
Hydrogen sulphide	19
Project description	21

List of abbreviation	23
Chapter two - Results and discussions	24
CcP: Nitric oxide Biosensor	24
Absorption spectra and F.R.E.T. system	24
Fluorescence spectroscopy	27
NO affinity and Determination of K_d	30
Determination of NO binding kinetics	33
Selectivity and Control experiments	36
Immobilization in Sol Gel matrices	41
Application of the CcP_Atto620 NO Biosensor in <i>Arabidopsis thaliana</i> suspended cells	45
Heavy metal stress and monitoring of the NO production	45
Internal Cd^{2+} quantification	49
NO Quantification in <i>Arabidopsis thaliana</i> suspended cells	50
Myoglobin: Hydrogen sulphide biosensor.....	52

Absorption spectra and F.R.E.T. system	52
Immobilization into sol gel matrices	57
Chapter three - Conclusions	59
CcP_Atto620. The Nitric oxide biosensor	59
CcP_Atto620 NO Biosensor in <i>Arabidopsis thaliana</i> suspended cells	61
Myoglobin as a Hydrogen sulphide biosensor	63
Chapter four - Materials and Methods	64
Extraction and purification proteins	64
Protein labelling	64
Forster radius calculation	65
Absorption and fluorescence measurements	66
Release NO product and NO saturated solution	67
H ₂ S and (NH ₄) ₂ S saturated solutions o synthesis	68
Sol Gel matrix	68
Cells cultures and treatments	69
Suspended cells and heavy metal stress in close system	70

Internal Cd ²⁺ Quantification	70
H ₂ S measured and NO Quantification by Fluorescence Analysis	71
References	72

Chapter one - Introduction

Abstract

In recent years the field of chemical sensors and optical biosensors has been developed considerably. A biosensor is a device composed of a biological component (Borisov and Wolfbeis 2008) that interacts with a target analyte (ion, molecule, etc.), in a highly specific and selective translation of a chemical or biological response into a measurable physical signal. A biosensor offers several advantages. In fact, it is highly specific with reproducibility in measurements, and a rapid response. The decisive impetus to this development was initially received by the medical industry. However, other sectors such as food quality control as well as environmental monitoring have expressed a recent growing interest in this area. There is therefore a need for a multidisciplinary approach to the subject.

Optical Biosensors

Optical biosensors are devices that offer a wide spectrum of advantages over traditional sensing systems, e.g. small size, longer lifetime and immunity to electromagnetic interference. When the binding of a target molecule is accompanied by a unique change in the spectroscopic characteristics (usually absorption or fluorescence) of the biomolecules this provides the basis for developing an optical biosensor (fig.1). A biomolecule suitable for implementation in a biosensor must possess two main characteristics:

- specificity of binding the analyte
- proper signal transduction

Unfortunately, the terminology on biosensors is not systemic. Doctors tend to refer to “biosensors” as solid-phases-based diagnostic devices such as those for glucose, pregnancy markers, or cardiac markers. They should be referred to as test strips. Others, (mainly bioorganic chemists) often refer to molecular bioprobes as biosensors. (Borisov and Wolfbeis 2008)

Biosensors are classified according to the nature of the interaction, they establish with the analytes as well as the type of signal that reaches the transducer as a result of these interactions (electrochemical or optical biosensors).

The biosensors can also be divided into two groups:

- Catalytic Biosensors
- Affinity Biosensors

The first makes use of biocomponents that are capable of recognizing (bio)chemical species and transforms them into a product through a chemical reaction. This type of biosensor is represented mostly by enzymatic biosensors, which make use of specific enzymes or their combinations. Many whole-cell biosensors also rely on biocatalytic reactions. More recently, catalytically active polynucleotides (DNAzymes) have been used too. This type of biosensor also includes biosensors based on the measurement of the inhibition rate of a catalytic reaction by an inhibitor such as a heavy metal ion or a pesticide. Catalytic whole-cell sensors are often used to sense sum parameters such as toxicity, antibiotic activity, or cell viability. The latter may use of the specific capabilities of an analyte to bind to a biorecognition element. This group can be further divided into immunosensors (which rely on specific interactions between an antibody and an antigen), nucleic acid biosensors (which make use of the affinity between complimentary oligonuclotides), and biosensors based on the interaction between an analyte (ligand) and a biological receptor. Some whole-cell biosensors act as recognition elements responding to (trigger) substances by expressing a specific gene. (Borisov and Wolfbeis 2008)

Our goal is the development of optical affinity biosensors using heme proteins.

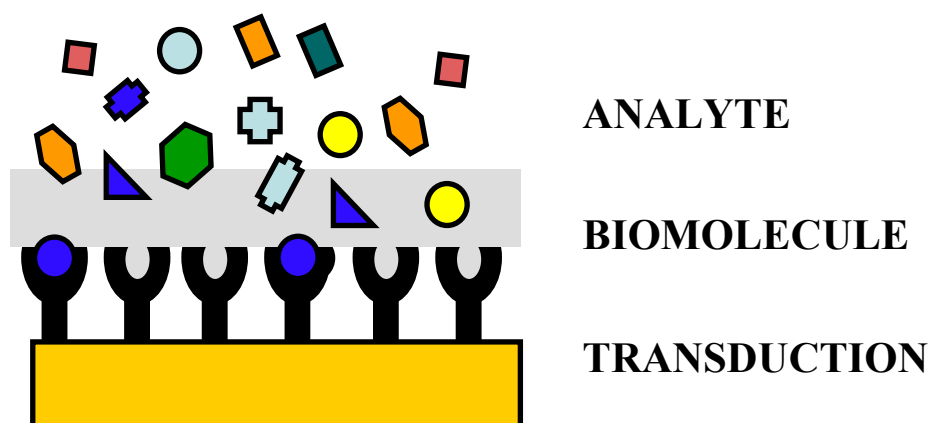


Fig. 1 Example design of an optical biosensor

The proteins used in this work as molecular recognition elements for toxic gases

Heme proteins

Hemeproteins, or heme proteins, are metalloproteins containing a heme prosthetic group, either covalently or noncovalently bound to the protein itself. Nature uses heme proteins to carry out a myriad of different biological functions. Since their discovery, the structural and functional aspects of heme proteins have fascinated biochemists and synthetic chemists alike (Pond et al. 1999) (Paoli M. et al. 2002). Nature has evolved heme binding sites within a variety of protein scaffolds (Martin et al. 1998) in order to carry out various task such as diverse tasks as electron transfer, substrate oxidation, metal ion storage, ligand sensing, (Chan M.K.J. 2000;Chan M.K.J. 2001) and transport.

The heme proteins involved in electron transfer were initially described in 1884 by MacMunn as respiratory pigments (myohematin or histohematin)(McMunn C.A. 1886). In the 1920s, Keilin rediscovered these respiratory pigments and named them “cytochromes” or “cellular pigments”, (Kellin D. 1925) and then classified them on the basis of the position of their lowest energy absorption band in the reduced state, as cytochromes *a* (605 nm), *b* (565 nm), and *c* (550 nm).

There are many heme groups in nature. Heme *b*, also called protoheme. All the porphyrins are synthesized in vivo as the free base forms before incorporation of the iron(II) by the enzyme ferrocheletase.(Sellers et al. 2001;Wu et al. 2001). Additionally, heme *b* serves as the structure from which hemes *a* and *c* are biosynthetically derived.

Oxidation/reduction enzymes and metalloproteins represent more than 40% of the IUBMB classified proteins. They are not only vital to biological energy conversion in photosynthesis and respiration, but are also critical to a growing number of signalling processes governing gene regulation and expression. (Kennedy M.L and Gibney B.R. 2001)

Heme proteins are uniquely adapted to binding the important diatomic molecules O₂, NO and CO. (Spiro T.G. and Jarzecki A.A. 2001)

Hemes remain one of the most visible and versatile classes of cofactor used in biology. In fact, heme proteins are an integral component in numerous vital biological processes including steroid biosynthesis, aerobic respiration, and even programmed cell death. Found in both archaeas as well as higher organisms, the ubiquity of heme proteins further emphasizes their operational importance within biological systems.

This therefore makes heme protein an excellent candidate for optical biosensor development.

CcP (Cytochrome *c* Peroxidase)

Cytochrome *c* Peroxidase (CcP) is a water-soluble heme-containing enzyme of the peroxidase family that takes reducing equivalents from cytochrome *c* and reduces hydrogen peroxide to water. The yeast enzyme is a monomer of molecular weight 34,000 Da, located in the inter-membrane space of yeast mitochondria, containing 293 amino acids. It also contains a single noncovalently bound heme *b* (fig.2).

The metal center is composed of one atom of iron penta-coordinated with the sixth coordination site vacant and free to bind nitrogen monoxide. The resting state CcP (Fe^{III}) contains a non covalently bound heme with a five-coordinate, high spin iron ($S=5/2$). The protein used in this project was a yeast extract and expressed in *E. coli*.

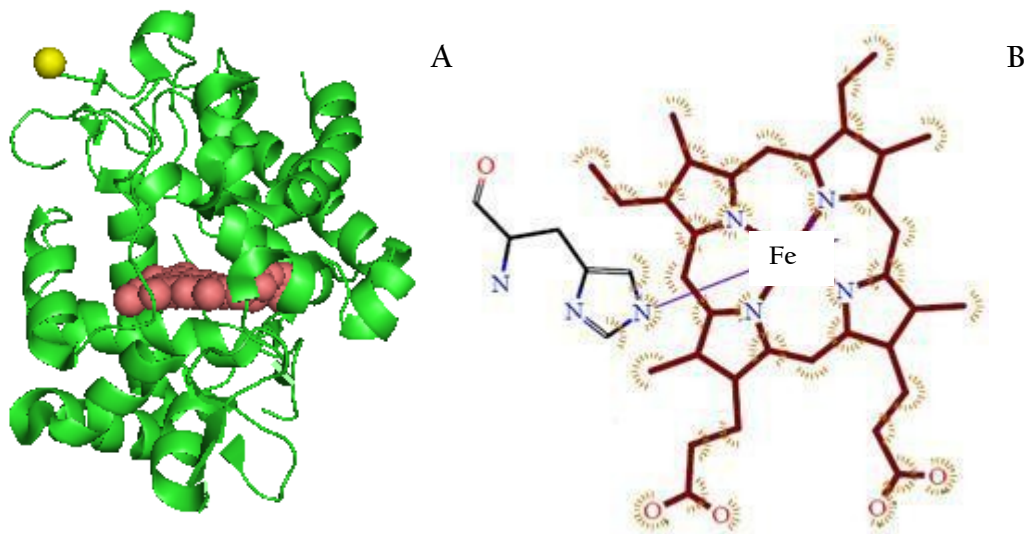


Fig. 2 A. Structure of CcP showing the heme (red spheres) and Leu 1 (yellow). Leu 1 corresponds to the attachment point of the label. The structure has been obtained from the PYMOL programme using the reported X-ray diffraction structure of CcP (PDB 1ZBY). B. Heme group.

Mb (Myoglobin)

Myoglobin (Mb) is a single chain globular protein of 153 amino acids, containing a heme prosthetic group with iron in the center. It has eight alpha helices and a hydrophobic core (fig.3). It has a molecular weight of 16,700 Da, and is the primary oxygen-carrying pigment of muscle tissues. This protein does not exhibit cooperative binding of oxygen, since positive cooperativity is only a property of multimeric/oligomeric proteins only. On the other hand, the binding of oxygen by myoglobin is unaffected by the oxygen pressure in the surrounding tissue. High concentrations of myoglobin in muscle cells allow organisms to hold their breaths longer. Diving mammals such as whales and seals have muscles with a particularly high myoglobin abundance.

Myoglobin was the first protein to have its three-dimensional structure revealed. In 1958, John Kendrew and associates successfully determined the structure of myoglobin by high-resolution X-ray crystallography. John Kendrew shared the 1962 Nobel Prize for chemistry with Max Perutz for this discovery. The protein used in this project was purchased from Sigma-Aldrich.

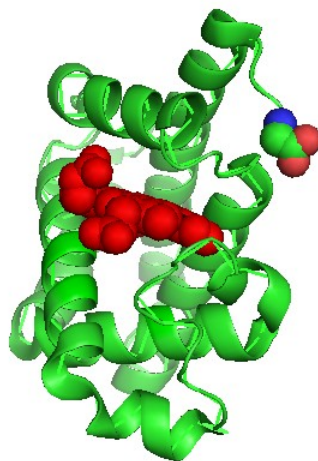


Fig. 3 Myoglobin from horse skeletal muscle with the heme group (red spheres)

Fluorescence

Fluorescence can be seen as an energy dissipation process of optically excited atoms or molecules. In fact, when electrons move from a higher energy state to a lower one, the energy recovered can be issued in the form of electromagnetic radiation. Once the molecule has absorbed the incident radiation back to the ground state, the dissipation of the energy received can occur in two ways:

1. through encounters with other molecules such as solvent, or through motions that occur in solids, the energy emitted as heat, allowing the surrounding molecules to perform vibrations, rotations and translations, in fact, the molecule can transfer energy turns into kinetic energy, vibrational energy, etc. with the effect still being a heat increase;
2. in the molecule where it undergoes a radiative decay, with energy excess being released as photons, resulting in a spontaneous emission event which can be fluorescence or phosphorescence.

Fluorescence is the phenomenon in which a molecule struck by a light radiation at a certain wavelength (frequency of excitation) emits a wavelength more than another (frequency of issue). The fluorescent molecules (fluorophores, fluorochromes or fluorescent dyes) absorb light in a lower region of the spectrum (fig. 4 upper) and thereby emit light (photon energy) "Fluorescent" in an upper region of the spectrum at a higher wavelength (λ). In fact, after this absorption, outer orbital electrons move from one energy level to a higher (excited) one, where they stay at the top level is very short, about billionths of a second, after which the electrons return to the original energy level release

energy in the form of electromagnetic radiation (Photon emission)(fig.4 lower)(Lakovicz J.R. 1996). Since energy efficiency is never 100%, the radiation released is at a higher wavelength and thus less energy than excitation energy. The emission is shifted towards the red region than excitement because it is the area of lower energy. This phenomenon is known as the Stokes shift (Lakovicz J.R. 1996). Each molecule has a specific emission spectrum, with molecules that are able to emit light in a particularly efficient way when excited being defined as fluorophores.

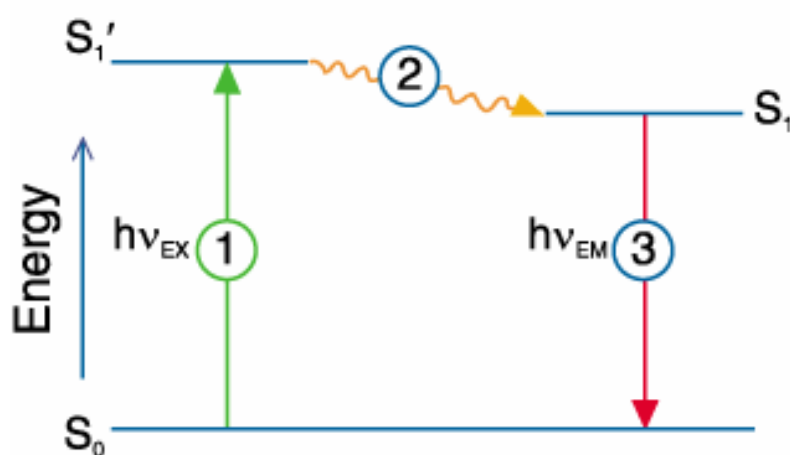
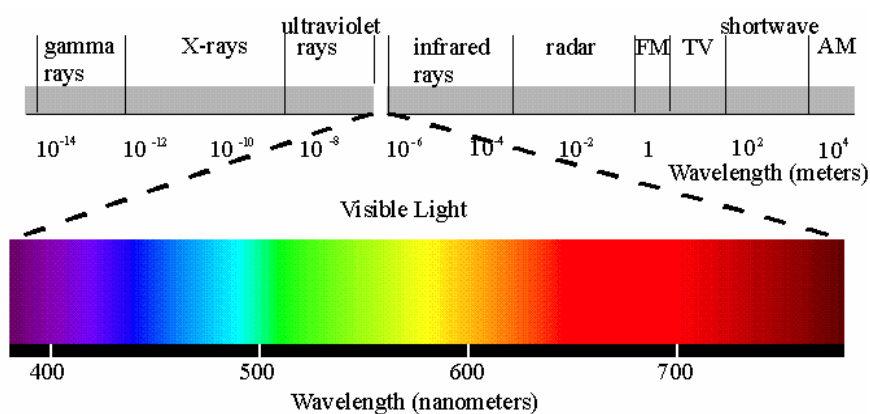


Fig. 4 Upper. Visible spectral analysis by flow cytometry. Lower. Jablonski diagram. Describes the phenomenon of excitation of a dye and subsequent fluorescence emission.

F.R.E.T. (Forster resonance energy transfer)

Forster resonance energy transfer (FRET) is a process by which a fluorophore (the donor) in an excited state transfers its energy to a neighboring molecule (the acceptor) by nonradiative dipole-dipole interaction (Forster T. 1948; Lakovicz J.R. 1999). Although it is not necessary, in most cases the acceptor is also a fluorescent dye, also in this case. In this case, FRET also stands for fluorescence resonance energy transfer. This application of fluorescence is based on the fact that energy absorbed by a chromophore can be transferred to another chromophore yielding an increase of its fluorescence intensity, depending on the distance. (Stryer and Haugland 1967)

The excitation energy from a fluorescent donor molecule is transferred by a radiationless process to an acceptor chromophore, resulting in a decrease of donor fluorescence. The probability of this transfer (FRET efficiency, E) drops off as the inverse sixth power of the distance between donor and acceptor, R . Furthermore, the transfer efficiency (E) is a direct measurement of the fraction of photon energy absorbed by the donor that is transferred to an acceptor. Since E depends on the inverse of the sixth power of the distance r between the two fluorophores, $E = R_0^6 / (R_0^6 + r^6)$, FRET has become the technique of choice to observe protein-protein interactions as well as measure the distances between fluorophores (Clegg R 1996; Stryer 1978; Stryer and Haugland 1967). R_0 is known as the “Forster distance” and represents a characteristic parameter of every dye pair defining the distance at which the efficiency is 50%. (Berney C. and Danuser G. 2003). Thus, if R_0 is known, FRET efficiency can be used to estimate the donor-acceptor distance, R .

In addition, $R_0^6 \sim \kappa^2 \cdot J(\lambda)$, where κ^2 is an orientation factor and $J(\lambda)$ is the overlap between the donor emission spectrum and acceptor absorption spectrum (fig.5).

In most cases fluorescent labels are used both as the donor as well as acceptor for FRET. However, the prosthetic group of a protein itself can also act as an acceptor. (Kuznetsova et al. 2006). In order to know the energy involved in the process, the transfer efficiency will be used to measure the performance of the biosensors.

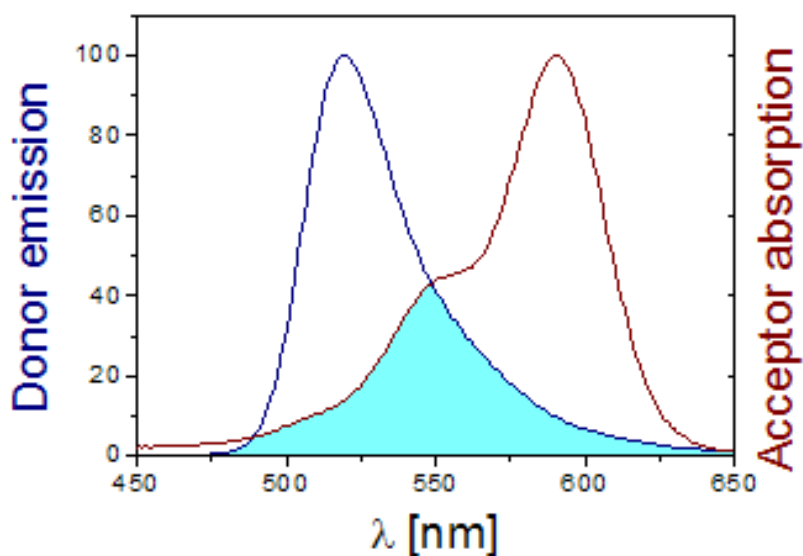


Fig. 5 Forster Resonance Energy Transfer, overlap between emission and absorption spectrums

The analytes under investigation: NO and H₂S

Nitric oxide

In 1992, NO was recognized by *Science* magazine as the 'Molecule of the year'. (Koshland, Jr. 1992). This reflected the discovery that NO plays a crucial role in a variety of biological processes (E.Culotta 1992;Koshland, Jr. 1992). Further investigations led to the finding that NO is a multifunctional effectors in numerous mammalian physiological processes, including the relaxation of smooth muscle, inhibition of platelet aggregation, neural communication and immune regulation (Schmidt and Walter 1994). At micro molar concentrations NO can lead to carcinogenic and neurodegenerative disorders (P.K.Lala 1998;Thomsen and Miles 1998).

Studies of NO chemistry have contributed to an understanding of NO signaling mechanisms that are achieved through its interaction with targets via a rich redox and additive chemistry (Stamler et al. 1992;Stamler 1994).

In 1998, three NO research pioneers (Robert F. Furchgott, Louis J. Ignarro and Ferid Murad) won the Nobel Prize for "Physiology or Medicine" for their discoveries relating to "the nitric oxide as a signaling molecule in the cardiovascular system".

The use of NO is not confined to the human health and the animal kingdom, in fact nitric oxide is a gaseous reactive molecule with a pivotal signaling role in many developmental and response processes (Besson-Bard et al. 2008;Neill et al. 2003).

The universal and unique role of the free radical NO as a biological signalling molecule is based on its physico-chemical properties which determine the mechanisms of the interaction with its targets and the nature of its movement.

Its hydrophobicity enables not only a rapid diffusion in a physiological environment but also the unhindered passage through lipid membranes, such as cell plasma membrane. NO is a free radical lipophilic diatomic gas under atmospheric conditions. Compared to other free radicals, NO has a rather low overall reactivity. It reacts predominantly with molecules that have orbitals with unpaired electrons, which are typically other free radicals or transition metals like heme iron.

NO is an ubiquitous by-product of high temperature combustion (Ball et al. 1999) as well as one of the hazardous exhaust gases generated by motor vehicles (Dooly et al. 2008; Thomsen and Miles 1998). Emissions of these gases cause local and global environmental problems such as acid rain, greenhouse effects, destruction of the ozone layer and air pollution.

NO has created a great deal of interest in environmental science for many years, particularly due to its dual role in the catalytic formation and destruction of ozone (O_3). In NO-rich air, such as those encountered in industrialized regions, reactive nitrogen oxides ($NO_x = NO + NO_2$) also play a key role in the chemistry of the lower atmosphere; NO is important for the atmospheric radical balance as well as the generation of photo-oxidants (Wildt et al. 1997).

Sources of NO_x may be both anthropogenic and natural. NO_x concentrations may range up to 100 ppb in the air over industrialized (fossil fuel combustion) areas (Wildt et al. 1997). The release of NO from natural sources is mainly attributed to the activity of soil micro-organisms.

In the last decade, many devices were implemented to monitor NO. Real-time measurement of NO in biological preparations is often highly desirable. However, the instability of NO in aqueous solution and its high reactivity with various other species can cause difficulties in its measurement depending on the detection method employed (Lamattina et al. 2003).

Different techniques and methodologies can be used in measuring NO. It is possible to carry out:

- direct measurements (gas chromatography, mass spectrometry, electrochemical, etc)
- indirect measurements (Griess Reagent, 4,5-diaminofluorescein DAF-2, etc)

In 1998 the first example of a fluorescence-based system for sensing NO was reported. The method made use of cytochrome c' immobilized on gold nanobeads as the sensing material. The sensor operates in a reversible way and the reported detection limit was 20 μM (Barker et al. 1998). One year later the same group improved the performance of this sensor by employing fluorescent ratiometric measurements. The improved sensor consisted of fluorescently labeled cytochrome c' incorporated within polystyrene nanobeads labeled with a fluorescent reference dye, whose emission allowed ratiometric (two wavelengths) measurements. Compared to the previous construct, the detection limit of the sensor was lowered to 8 μM (Barker et al. 1999a).

A relevant application of this NO sensing system is the measurement of NO produced by macrophages (Barker et al. 1998; Barker et al. 1999b). The system relies on a FRET-based (Förster Resonance Energy Transfer) mechanism by which the dye fluorescence is attenuated as the protein binds NO. The observed fluorescence changes were ascribed (Barker et al. 1998) to conformational alterations in cyt c' induced by NO binding. This type of sensor is commonly referred to as a “turn-off” sensor since it exploits the quenching of the dye fluorescence upon analyte binding. FRET-based ratiometric fiber-optic NO sensors were prepared with the heme domain of soluble guanylate cyclase (Barker et al. 1999b). They also belong to the family of the “turn-off” sensors, and function in a similar way to the biosensors prepared with cytochrome c'. With a

genetically encoded fluorescent indicator, NOA-1, the physiological nanomolar dynamics of NO in single living cells have been reported as detectable (Sato et al. 2005). The sensing system is suitable for monitoring NO release by endothelial cells, neurons and macrophages (Sato et al. 2005).

Kojima *et al.* in 1998 developed fluorescence probes based on the fluorescein chromophore which were able to detect intra- as well as extra-cellular NO (Kojima et al. 1998). The most common probe up to now is 4,5-diaminofluorescein (DAF-2). DAF-2 which itself shows only low fluorescence, reacts in the presence of oxygen with NO to form the highly fluorescent triazolofluorescein (DAF-2T). In particular DAF-2 reacts with NO derived species (notably N_2O_3) resulting from NO oxidation to yield a triazole fluorescent derivative (DAF-2T). DAF-2 is an impermeable. To order to measure intracellular NO, cells can be loaded with the membrane permeable DAF-2 diacetate (DAF-2DA) which can be taken up by the cells and hydrolyzed by cytosolic esterases to re-form the membrane-impermeable compound DAF-2. This compound is largely used in literature, with it being an indirect measurement.

An application of the labeled -CcP system as NO biosensor: an example in vivo

In plants, NO can be synthesized via several routes, either enzymatically or by chemical reduction of nitrite. Nitrate reductase and a root-specific plasma membrane nitrite-NO reductase also utilize nitrites as a substrate. Although no plant NOS has been unambiguously identified yet, activity assays and pharmacological data suggests the existence of a NOS-like counterpart in plants. Depending on its concentration and possibly on the timing and localization of its production, NO can either act as an antioxidant or promote PCD, often in concert with ROS (Beligni et al. 2002;de Pinto et al. 2006;Delledonne et al. 2001). Extensive research has shown that NO plays a fundamental role in the hypersensitive response, but its involvement in other types of PCD, such as that resulting from mechanical stress and natural and cytokinin-induced senescence of cell cultures, has also been demonstrated (Carimi et al. 2005;Garces et al. 2001). Due to its participation in numerous biotic and abiotic responses, NO has been proposed as a general stress molecule (Gould et al. 2003). However, the mechanisms by which NO determines its effects are far from being completely explained, and a number of downstream signaling pathways, involving Ca^{2+} , cyclic GMP, and cyclic ADP-Rib, are involved (Besson-Bard et al. 2008;Neill et al. 2003). NO can also modulate biological responses by direct modification of proteins, reacting with Cys residues (S-nitrosylation), Tyr residues (nitration), or iron and zinc in metalloproteins (metal nitrosylation) (Besson-Bard et al. 2008).

The ability of plants to accumulate and metabolize atmospheric NO has been known for some time (Nishimura et al. 1986). Moreover, measurement of gaseous emissions from plants has shown that NO can be synthesized in plants, through both non-enzymatic and enzymatic reactions (Leshem and Haramaty 1996;Yamasaki 2000). Interestingly, studies carried out over the past few years

have shown that NO is at the heart of several physiological functions ranging from plant development to defense responses (Beligni and Lamattina 2000;Durner and Klessig 1999).

Therefore, the chemistry of NO is the most important determinant of its function in biological systems and may be separated into two basic categories, i) direct effects and ii) indirect effects, primarily based on the concentration of NO. (Wink and Mitchell 1998).

Arabidopsis thaliana is a small flowering plant that is widely used as a model organism in plant biology. Arabidopsis is a member of the mustard (Brassicaceae) family, which includes cultivated species such as cabbage and radish. Arabidopsis is not of major agronomic significance, but it offers important advantages for basic research in genetics and molecular biology. (www.arabidopsis.org)

Cadmium (Cd^{2+}) is a heavy metal with a long biological half-life, and its presence as a pollutant in agricultural soil is due mainly to anthropogenic activities. It is rapidly taken up by roots and enters the food chain, resulting in toxicity for both plants and animals (di Toppi and Gabbrielli 1999). Cd^{2+} inhibits seed germination, decreases plant growth and photosynthesis, and impairs the distribution of nutrients. Overall, the symptoms of chronic exposure to sublethal amounts of Cd^{2+} mimic premature senescence.

Cd^{2+} pollution is of major concern, since it hampers plant growth by triggering inhibition of photosynthesis and nitrogen metabolism and by decreasing water and mineral nutrient uptake. Moreover, Cd^{2+} accumulation in crops compromises their commercial value and presents a potential risk to human health.

Although Cd^{2+} is an environmental threat, the mechanisms by which it exerts its toxic effects in plants are not fully understood. In plant cells, Cd^{2+} is believed to enter through Fe^{2+} , Cd^{2+} , and Zn^{2+} transporters/channels (Clemens 2006). Once

in the cytosol, Cd^{2+} stimulates the production of phytochelatins (PCs), a glutathione-derived class of peptides containing repeated units of Glu and Cys, which bind the metal ions and transports them into the vacuole (di Toppi and Gabbrielli 1999). There is a great deal of evidence exists that high (millimolar) concentrations of Cd^{2+} induce reactive oxygen species (ROS) bursts in plants, which might have a role in signaling and/or degenerative steps leading to cell death (Piqueras et al. 1999). Treatment with a lower, nontoxic Cd^{2+} concentration also caused an increase in ROS production in pea (*Pisum sativum*) leaves and roots (Rodriguez-Serrano et al. 2006) as well as *Arabidopsis* (*Arabidopsis thaliana*) cell cultures (Horemans et al. 2007) (De Michele et al. 2009).

NO was shown to participate in a wide spectrum of physiological processes, including germination, root growth, gravitropic bending, control of the timing of flowering, stomatal closure, and growth regulation of pollen tubes (Besson-Bard et al. 2008; Wilson et al. 2008). Furthermore, NO has also been implicated in the plant adaptive response to biotic and abiotic stresses, notably by acting as a signaling molecule (Delledonne 2005; Gould et al. 2003).

Several studies have investigated NO production during plant exposure to metals, including aluminium and iron (Gould et al. 2003).

NO production has been detected in *Arabidopsis* cell suspensions upon iron supply (Arnaud et al. 2006). In this context, NO appears to be a key element in the signal transduction pathway leading to the increase of the iron-storage protein ferritin at both mRNA and protein levels (Arnaud et al. 2006; Murgia et al. 2002).

The possibility that plant exposure to Cd^{2+} might modulate NO production has been reported, but conflicting results have been published regarding the impact of Cd^{2+} on NO production. Depending on the biological model, either Cd^{2+} mediated induction (Kopyra and Gwozdz 2003) or inhibition (Rodriguez-Serrano et al. 2006) of NO production has been reported (Besson-Bard et al.

2009). In the corresponding studies, the treatment of plants with artificially generated NO was shown to protect plant tissues against the oxidative damage triggered by Cd²⁺ by promoting the scavenging of reactive oxygen species (ROS) directly through chemical processes or indirectly via the activation of ROS scavenging enzymes (Kopyra et al. 2006; Noriega et al. 2007). Although informative, these studies did not take into account the possibility that NO might be endogenously produced in response to Cd²⁺ and, therefore, might exert specific roles in this particular physiological context. (Besson-Bard et al. 2009)

Hydrogen sulphide

Hydrogen sulphide (H₂S) is a colorless gas with a very characteristic odor of rotten eggs which can be perceived organoleptically at concentrations as low as 0.025 ppm (Hirsch 2002).

It is considered one of the most dangerous environmental toxic and crude metabolic poisons. It is more toxic than hydrogen cyanide and exposure to as little as 300 ppm in air for just 30 min can be fatal in humans. (Li L. and Moore P.K. 2007; Strianese et al. 2010b). Nevertheless, hydrogen sulphide can also produce the deterioration on the normal function of several organs in the body including eyes, lungs, olfactory parts, nervous system, heart, brain, gastrointestinal system, and liver (Fuller D.C. and Suruda J. 2000).

H₂S is one of the biologically active gases that occur naturally in the body. This molecule is synthesized by enzymes and has physiological and/or pathophysiological functions within the body (Li L. and Moore P.K. 2007). In the cardiovascular system, H₂S relaxes vascular smooth muscle and inhibits smooth muscle cell proliferation. Thus, it plays a role in controlling blood pressure. It is an important factor in the development of some vascular diseases. In particular,

its deficiency can create a predisposition to vasoconstriction and hypertension. In addition it acts as a neuromodulator in the central nervous system. (Chen C.Q. et al. 2007;Li L. and Moore P.K. 2008;Reiffestein R.G. and Hulbert W.C. 1992)

This gas can be found in several natural sources: volcanic gases, marshes, sulfur springs, putrefying vegetable and animal matter. It is also present as an industrial by-product, coming from some petroleum refining, natural gas plants, coke oven plants, knot pulp mills, and tanneries (Choi M.M.F. and Hawkins P. 2003). This gas is a particular hazard for workers in the oil drilling and refining industries.

The interest in the detection of hydrogen sulphide arises from the detrimental effects that exposure to this gas has in areas such as: health, environment, and industrial facilities care (J.A.Kramer 1992).

The most common approaches for H₂S detection are based on electrochemical and chromatographic techniques (Choi M.M.F. and Hawkins P. 2003). More recently, two methods based on polarography and carbon nanotubes coupled with a Raman and/or a confocal laser have shown promising results (Doeller J.E.et al 2005;Wu X.C. et al. 2007)

While each technique has its own advantages, there remains a need for simplicity in order to implement cheap H₂S sensors that can be used repeatedly. With fluorescence-based methods it is possible, in principle, to develop such a sensor. Commonly used dye indicators contain Hg complexes so as to exploit the affinity of sulphide ions to the Hg ion. In 1999 a dye containing a complex of Hg(II) and 2,2'-pyridylbenzimidazole with a detection limit of 4ppb of H₂S was reported (Rodriguez-Fernandez J et al. 1999). In this case the fluorescence depends on the formation of a species formed upon release of HgS, meaning that the H₂S is detected in an indirect way. A different dye tetraoctylammonium fluorescein mercury (II) acetate (TOAFMA) immobilized in ethyl cellulose (Choi M.M.F. and Hawkins P. 1997) and on PVC (Choi M.M.F. and Hawkins P.

2003) was reported as a H₂S sensor. In 2009 a small MW zinc complex was reported as a fluorescent sensor for H₂S detection (Galardon et al. 2009). As they claim, the strong point of this sensing system is its (partially) aqueous solubility and its selectivity against other thiols (Galardon et al. 2009).

Project description

The aim of the work was to develop cheap, reliable and sensitive biosensors based on fluorescence. We have investigated the use of proteins provided by a porphyrin ring (heme) such as Cytochrome c Peroxidase as a recognition element that allows for the detection of nitric oxide (NO) and Myoglobin from horse skeletal muscle in order to develop a biosensor capable of detecting hydrogen sulphide (H₂S). Since these gases affect human health, we tried to develop molecular systems useful to identify and quantify them in the environment.

These optical biosensors were developed using a FRET approach. The first goal was the development of an optical biosensor which was both easy to use as well as cheap.

Currently, there is a great deal of interest in NO, with a pressing need for methods capable of detecting NO in aqueous and gaseous media (Boon and Marletta 2006).

At present, the available technologies to monitor NO levels are based on chemiluminescent instrumentation (Kikuchi et al. 1993), amperometry (Mao et al. 1998), EPR spectroscopy (Kotake et al. 1996), colorimetric assays or porphyrin based fluorescent compounds (Lim and Lippard 2004).

Since each technique has its own advantages and disadvantages (Boon and Marletta 2006) (Nagano and Yoshimura 2002) (Lim and Lippard 2007) there is large space to implement, cheap NO sensors that can be easily used repeatedly and routinely (Franz et al. 2000). Fluorescence-based methods can, in principle, avoid some of the limitations of the existing methodologies.

Another goal of the project was the possibility to use the NO optical biosensor in an experiment *in vivo* in order to evaluate the possibility of using it in a real case. A part of this work was devoted to quantifying extracellular NO production.

In this work, suspension cell culture of *Arabidopsis thaliana* was exposed to Cd^{2+} (CdCl_2) as an "*in vivo*" system in order to monitor the extra cellular release of NO using a biosensor developed during the doctorate project.

The final aim of the project was the development of the H_2S optical biosensors. In fact, H_2S is considered one of the most dangerous environmental toxic and crude metabolic poisons and for this very reason developing a simple, selective and cost-effective sensing device for the monitoring H_2S is of significant importance. H_2S binding to Mb is possible and has been demonstrated in literature (Nicholls P. 1961). With fluorescence-based methods it is possible, in principle, to develop such a biosensor.

List of abbreviation

Atto620	Atto620 NHS-ester
BSA	Bovine serum albumin
CcP	Cytochrome c' Peroxidase
Cy3	Cyanine 3 NHS-ester
Cy5	Cyanine 5 NHS-ester
DAF-2	4,5-diaminofluorescein
E	Transfer efficiency
FRET	Forster Resonance Energy Transfer
H ₂ S	Hydrogen Sulphide
k _d	Dissociation constant
LR	Labeling ratio
Mb	Myoglobin
NO	Nitric Oxide
PCD	Programmed cell death
PVC	PolyVinyl chloride
R	Distance
R ₀	Forster radius
ROS	Reactive oxygen species
SR	Switching ratio
TMOS	Tetramethoxysilane

Chapter two - Results and discussions

CcP: Nitric oxide Biosensor

Absorption spectra and F.R.E.T. system

Cytochrome c Peroxidase is a soluble heme protein. It is a structurally, spectroscopically and functionally well characterized protein. Resting state CcP (Fe^{III}) contains a noncovalently bound heme with a five-coordinate, high spin iron ($S= 5/2$). The sixth coordination position is vacant, allowing ligands to bind (Barker et al. 1999b). Nitric oxide adducts of ferric Cytochrome c Peroxidase are stable and spectroscopically well characterized, as reported by Yonetani et al. already in 1972.

The overall properties of CcP make it an attractive candidate for developing a “turn on” (Lim and Lippard 2007) FRET-based NO biosensor. In particular, while the absorption spectrum of CcP exhibits a characteristic high spin marker band at 645 nm ($\epsilon= 3 \text{ mM}^{-1} \text{ cm}^{-1}$) (Pond et al. 1999), the binding of NO leads to the disappearance of this band (Yonetani et al. 1972) (see fig. 6A) (Strianese et al. 2010a). By attaching a fluorescent label to the protein, whose emission spectrum overlaps with the 645 nm band of the protein, this change in absorption upon NO binding can be translated into a change of fluorescence intensity of the label through a FRET mechanism. That is to say, when the protein is in the NO-free state, the label fluorescence becomes (partially) quenched as a result of FRET to the 645 nm band. As soon as NO binds to CcP, the latter band disappears and

the energy absorbed by the label is emitted as fluorescence, thus causing an increase in fluorescence. In this way the fluorescent dye acts as a passive “beacon” which is “off” in the NO-free state and “on” in the NO-bound state of the protein (fig 7). Two different labels, whose emission spectra overlap with the 645 nm spin marker band of CcP, were selected for this study: Cy5 and Atto620. The overlap of the 645 nm high spin marker band of CcP with the emission spectrum of either Atto620 or Cy5 can be judged from fig. 6B (Strianese et al. 2010a)

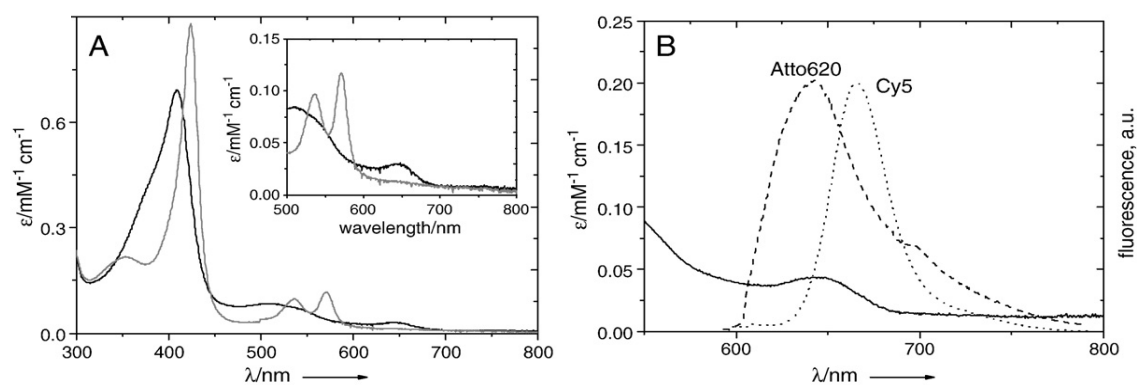


Fig. 6 Absorption spectrum of NO-free (black) and NO-bound (grey) CcP. Inset: 500–800 nm region of the spectrum with enlarged vertical scale showing the 645 nm high spin marker band of the NO-free CcP (black) and its disappearance in the NO-bound form (grey). B. Absorption spectrum of NO-free CcP (solid line) and emission spectra of Cy5 ($\lambda_{\text{max}}=665$ nm) (dotted line) and of Atto620 ($\lambda_{\text{max}}=645$ nm) (dashed line). All spectra measured at room temperature. Protein concentration: 8 μM in 100 mM potassium phosphate buffer (pH=6.8).

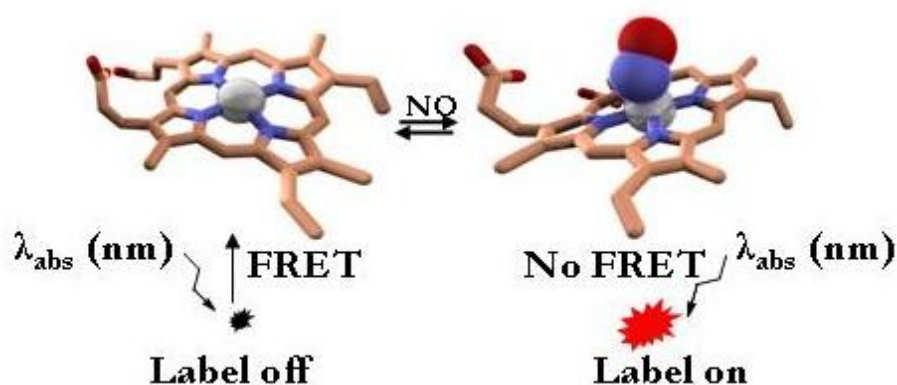


Fig. 7 Example of the “Beacon” mechanism. Switch off left side, switch on right side

CcP was labeled either with Atto620 or with Cy5. The pH of the labeling reaction was chosen so as to favour labeling of the N-terminus over lysine labeling. These conditions have been tested for the case of azurin, for which it was confirmed by electrospray MS that the label was exclusively present on the N-terminus (Kuznetsova et al. 2006). In the present case concentrations were chosen to ensure that the dye-to-protein ratio was less than 1. While a small dye-to-protein ratio affects only the sensitivity of the experiment, a ratio larger than 1 leads to ambiguities in donor-acceptor distances between the attached label and the prosthetic group of the protein. Moreover, it has been found that proteins labeled with multiple amino-reactive labels show a decrease in fluorescence due to mutual resonance energy transfer (Gruber et al. 2000). To check the number of label molecules per CcP, electrospray ionization mass spectrometry was performed on different Atto620 labeled CcP samples. Only peaks arising from unlabeled and singly labeled proteins were observed, showing that no CcP molecules with multiple labels were present in the samples (see fig.8) (Strianese et al. 2010a).

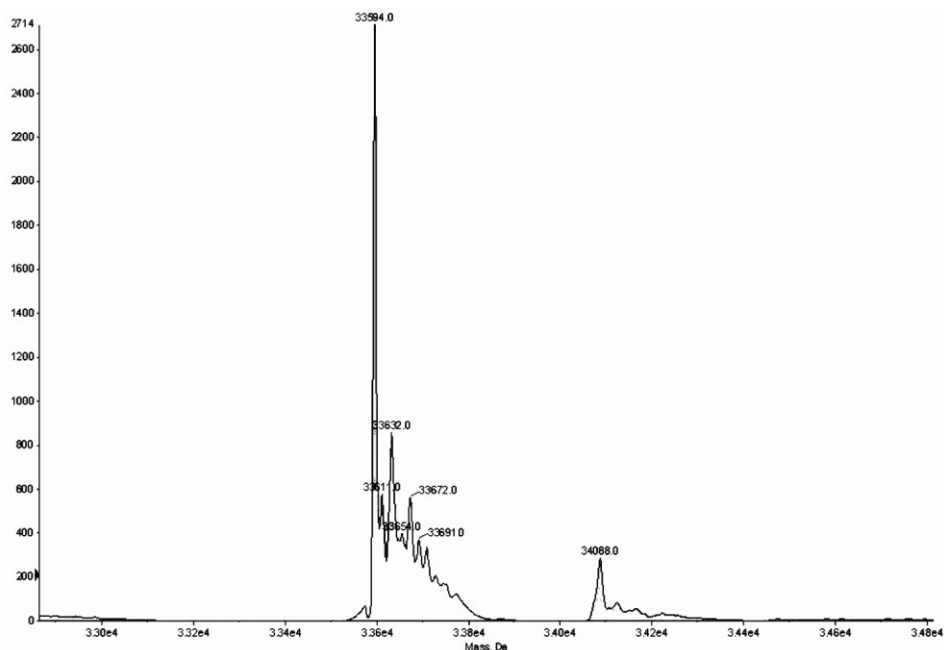


Fig. 8 Deconvoluted ESI mass spectrum of Atto620 labeled CcP, showing two species : native CcP and CcP with a single label. The 493 Da mass difference between the two species corresponds to the Atto620 label, as reported by the manufacturers

Fluorescence spectroscopy

To test the system, the fluorescence intensity of N-terminally labeled CcP was monitored as a function of time during a change from an NO-saturated to an NO-free environment. Fig. 9 shows a typical time trace of a solution containing 140 nM of dye-labeled CcP when excited at the absorption maximum ($\lambda=619$ nm) of the dye (Atto620).

Every experiment was brought in closed cuvette (mod. Hellma) to avoid contact with atmospheric O₂ and minimized its present in solution. In this particular experiment to add NO we used Mahma monoate (0,025M). Each cycle was started by adding NO to an end concentration of 360 μ M (i.e., in considerable excess over the CcP concentration) and completed by passing argon through the solution for the complete removal of NO (fig.9) (Strianese et al. 2010a).

The dye emission was followed at 640 nm. A fast increase in label emission was clearly observed upon each NO addition. When bubbling through argon to displace the NO, the fluorescence intensity of the label diminished again; the cycle could be repeated many times (at least four times).

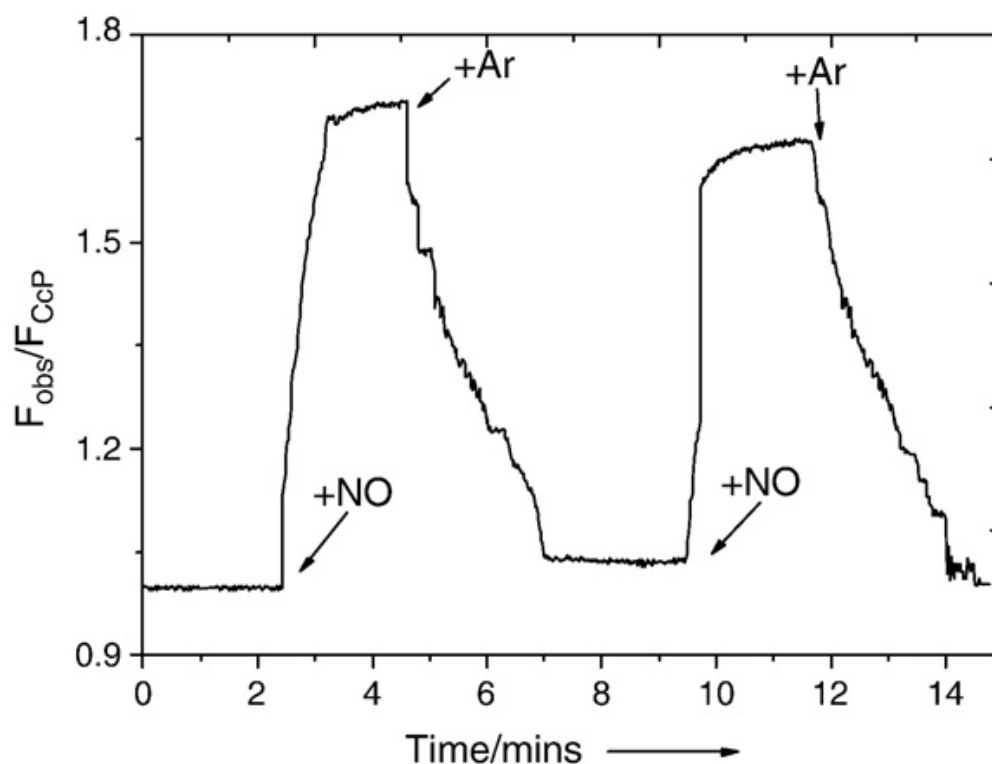


Fig. 9 Room temperature fluorescence intensity time trace observed at 645 nm (exc619 nm) of Atto620 labeled CcP, upon addition and removal of NO. The noise in the experimental trace after starting the bubbling of argon is due to the perturbation of the optical path of the measuring beam by the bubbling. Protein concentration: 140 nM in 100 mM potassium phosphate buffer (pH=6.8).

This finding showed that the NO binding process is reversible, which is crucial for practical sensing applications. The dye switching ratio (SR) defined by

$$SR = (F_{C_{cP-NO}} - F_{C_{cP}}) / F_{C_{cP-NO}} \quad (1)$$

in which $F_{C_{cP-NO}}$ and $F_{C_{cP}}$ are the emission intensities of the NO-bound and NO-free protein, is $45 \pm 5\%$. Of course SR ratio can vary depending on the type of dye used.

This can be compared with the theoretical value which is given by

$$SR = [E(CcP) - E(CcP-NO)] / [1 - E(CcP-NO)] \quad (2)$$

where $E(CcP)$ and $E(CcP-NO)$ are the theoretical FRET efficiencies in the NO-free and NO-bound state of CcP. E is given by $E = R_0^6 / (R_0^6 + R^6)$ (Lakovicz J.R. 1996) where R_0 is the Förster radius and R the distance between donor and acceptor. In the present case, the estimated Förster radii for FRET from Atto620 to the heme are 4.2 nm for the NO-free and 3.6 nm for the NO-bound state of CcP, while the donor-acceptor distance from Atto620 to the heme is 3.0 nm (as estimated from the crystal structure of CcP from baker's yeast [LZBY]).

This leads to theoretical transfer efficiencies of 0.88 for the NO-free state and 0.75 for the NO-bound state of CcP and a theoretical SR of 52%. Considering the uncertainties in the orientation factor, κ , (see Förster radius Eq.) and in the distance R , this value is in good agreement with the experimental value of $45 \pm 5\%$. It was found that the maximum and minimum fluorescence levels slowly decrease with the number of cycles the sample solution had gone through. This could be due to partial denaturation of the CcP after bubbling argon through the solution to displace the NO. In fact the fluorescence intensity of the construct after adding NO remained constant for hours when the solution was left standing. Under the same conditions also Cy5 labeled CcP exhibited a interesting SR of $40 \pm 5\%$. In this case the theoretically estimated R_0 values are 3.8 nm for the NO-free state and 3.3 nm for the NO-bound state and a theoretical SR of 56%. These experiments have been performed at pH 6.8 and provide a proof-of-principle for the proposed methodology.

NO affinity and Determination of K_d

To determine the binding affinity of CcP for NO, NO titrations of labeled CcP were performed while monitoring the fluorescence intensity of the labels (Figs. 10, 11). The relation between the observed fluorescence intensity, F_{NO} , and K_d is given by (Zauner et al. 2007):

$$F_{NO} = F_0 - \frac{(F_0 - F_\infty)[NO]}{[NO] + K_d} \quad (3)$$

where $[NO]$ is the concentration of free NO in solution and F_0 and F_∞ denote the emission intensities of the NO-free and NO-bound protein, respectively. According to Eq. (3) K_d is independent of the labelling ratio. A different labeling ratio is equivalent to introducing a scale factor for the fluorescence intensities which leaves Eq. (3) invariant. Since the protein concentrations used in the experiments were small compared to the NO concentrations, for practical purposes the free $[NO]$ could be set equal to the total amount of added NO and the data points in (figs. 11, 12) could be directly fitted to Eq. (3) resulting in a K_d of $9.4 \pm 0.5 \mu\text{M}$ for the Atto620 CcP system and of $12.0 \pm 2 \mu\text{M}$ for the Cy5 CcP construct. While we could not find literature data on the K_d for NO, the K_d values found here are in mutual agreement (Strianese et al. 2010a).

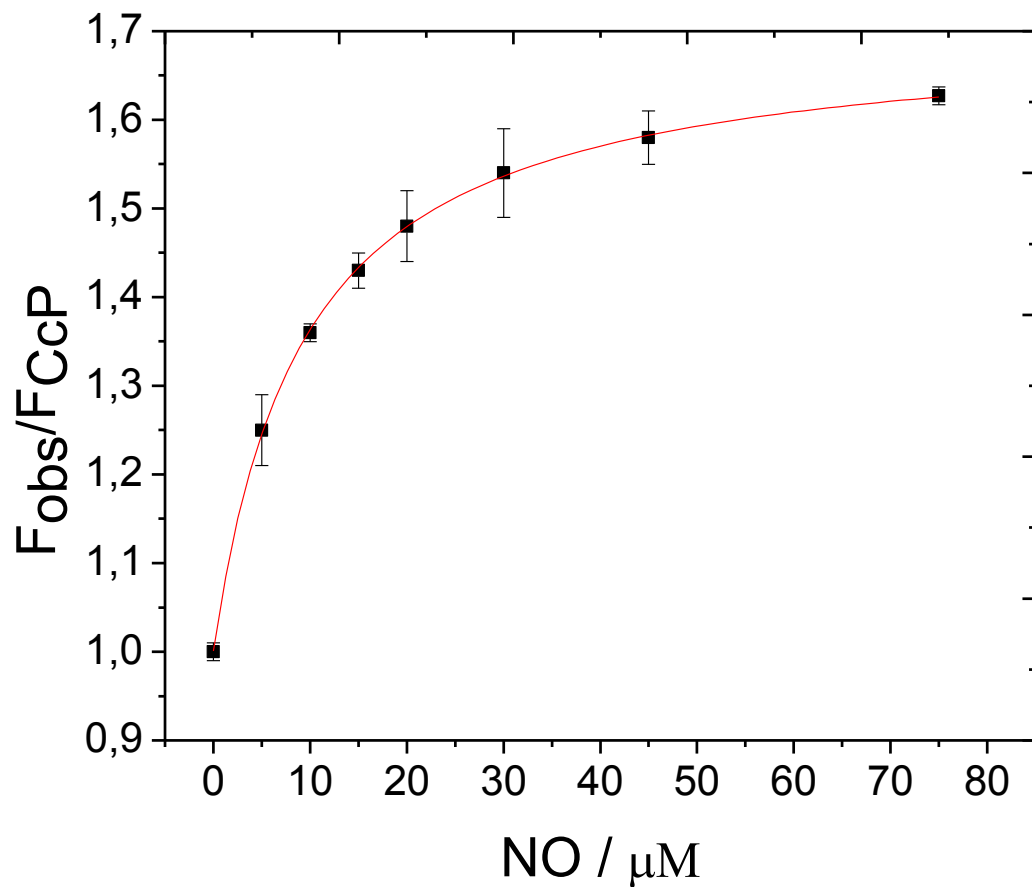


Fig. 10 Titration of CcP/Atto620 with NO monitored by the dye emission (645 nm). The fluorescence intensity of CcP/Atto620 normalized on the fluorescence intensity in the absence of NO is plotted versus the total NO concentration. The solid line represents the best fit to the data [(Eq.(4)] with $K_d = 9.4 \pm 0.2$. Protein concentration: 140 nM in 100 mM potassium phosphate buffer (pH = 6.8)

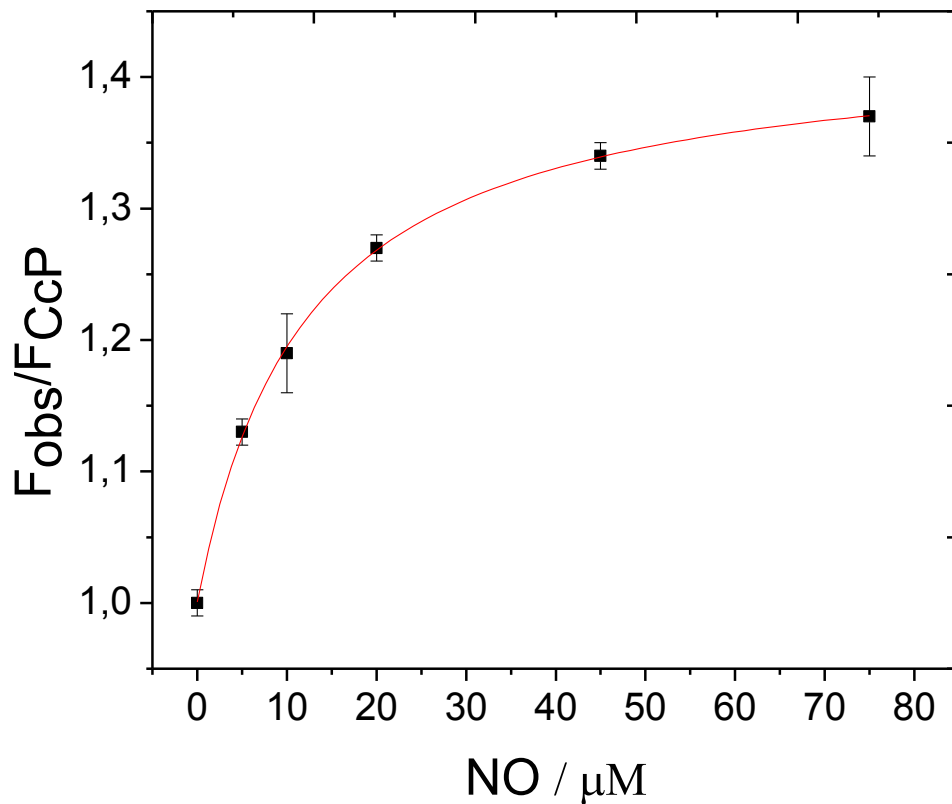


Fig. II Titration of CcP/Cy5 with NO monitored by the dye emission (665 nm). The fluorescence intensity of CcP/Cy5 normalized on the fluorescence intensity in the absence of NO is plotted versus the total NO concentration. The solid line represents the best fit to the data [(Eq.(4)] with $K_d = 12.0 \pm 0.6$. Protein concentration: 60 nM in 100 mM potassium phosphate buffer (pH =6.8)

Determination of NO binding kinetics

To assess the NO binding kinetics, we focused on the Atto620 CcP system. The fluorescence of the labeled CcP was measured as a function of time after adding various amounts of NO in the range of 1–75 μM . The fluorescence time traces (see Fig. 13) could be well fitted to an exponential function

$$F_{\text{obs}} = F_0 + \{F(t = \infty) - F_0\} \{1 - \exp(-k_{\text{obs}} * t)\} \quad (4)$$

When plotting the k_{obs} values as a function of the NO concentration, a linear dependence was observed. As an example, in fig. 12 the data are shown that were observed on a sample containing 20 nM of Atto620 labeled CcP.

When using for k_{obs} the expression $k_{\text{obs}} = k_{\text{off}} + k_{\text{on}} [\text{NO}]$ with k_{off} the rate of dissociation of the NO from the CcP/NO complex and k_{on} the second order rate constant for the association of NO and CcP, the following values could be extracted from the data in fig. 13:

$$k_{\text{off}} = 0.22 \pm 0.08 \text{ min}^{-1}$$
$$k_{\text{on}} = 0.024 \pm 0.002 \mu\text{M}^{-1} \text{ min}^{-1}$$

From these a value of $K_d = k_{\text{off}} / k_{\text{on}} = 9 \pm 3 \mu\text{M}$ is found in agreement with the K_d values derived from the NO titrations.

K_d is the key parameter for determining the sensitivity of the sensor. K_d is defined as $[\text{CcP}] [\text{NO}] / [\text{CcP-NO}]$ where $[\text{CcP}]$ is the concentration of the NO-free and $[\text{CcP-NO}]$ the concentration of the NO-bound CcP. The quantity by

which the sensitivity of the method can be judged is the ratio $[CcP]/[CcP-NO]$. This ratio varies strongly when the $[NO]$ is close to the K_d . Therefore, with the proposed biosensing system, NO can be easily detected and quantified in the concentration range of between 1 μM and 100 μM with simple fluorescence detection. For instance, with activated macrophages the transient NO concentration in cells or tissue is in the micromolar range (Barker et al. 1999a) (Barker et al. 1999b).

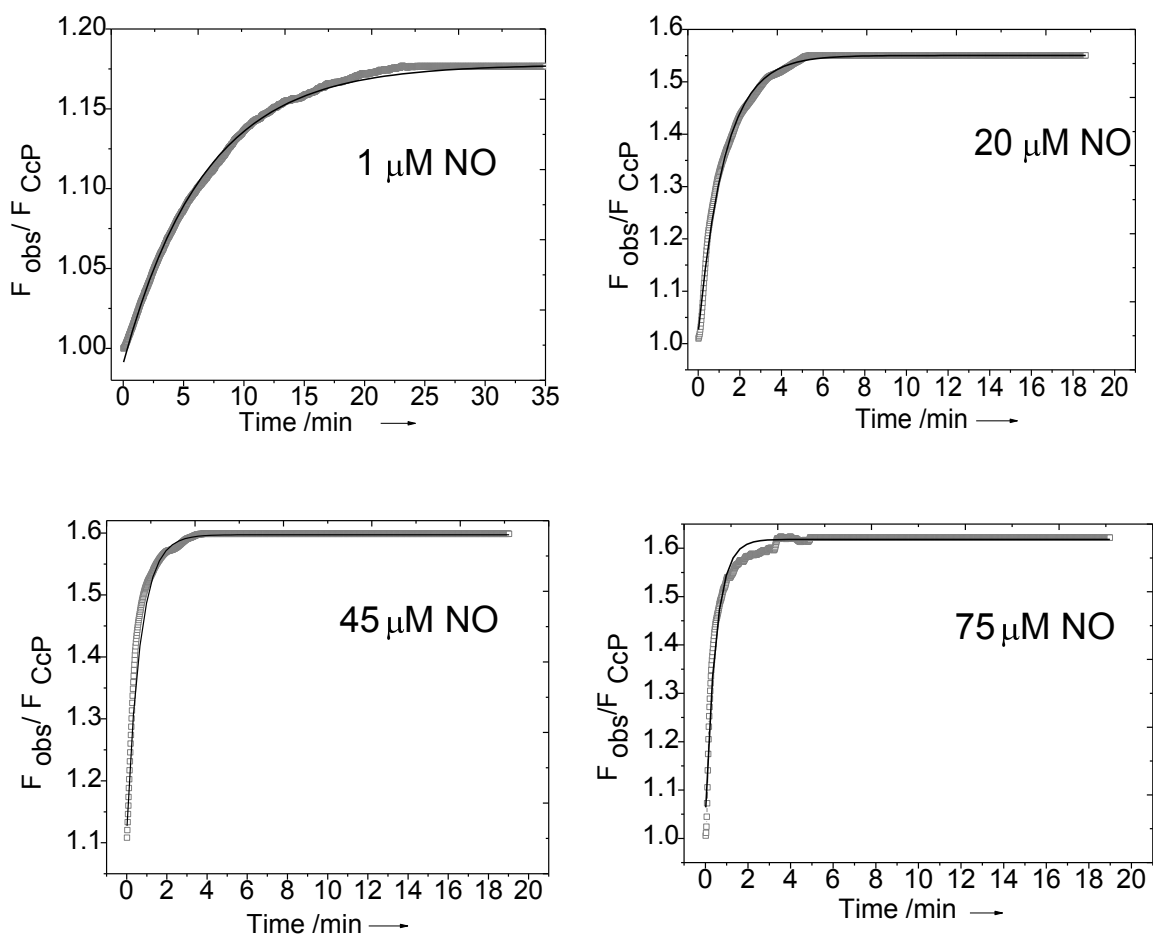


Fig. 12 Examples of the best fits to the kinetic traces observed after addition of various amounts of NO to a solution of 20 nM labeled CcP [eq. used for fitting: $F_{obs} = F_0 + \{F(t = \infty) - F_0\}\{1 - \exp(-k_{obs} \cdot t)\}$].

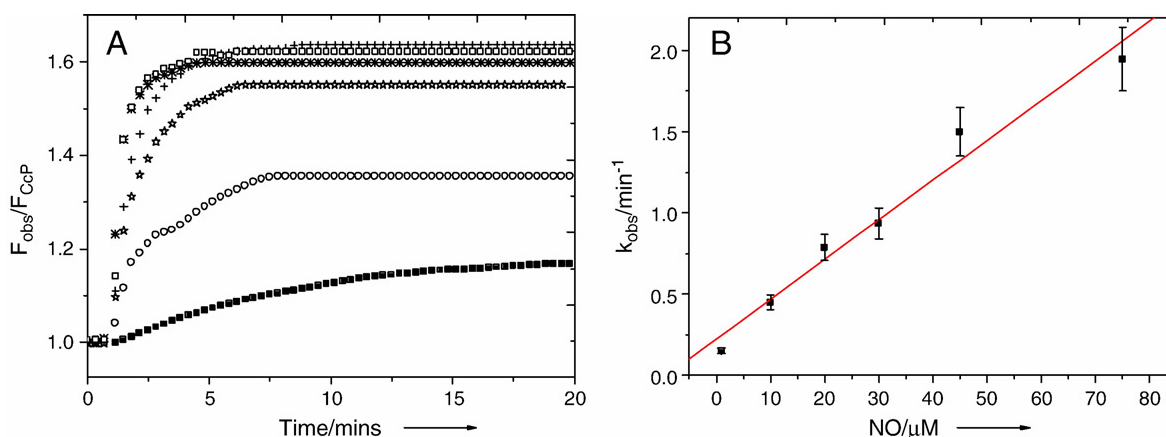


Fig. 13 A. Fluorescence time traces of Atto620 labeled CcP after addition of NO; end concentration of NO: 1 (■); 10 (◇); 20 (★); 30 (+); 45 (*); 75 (□) μM. The fluorescence time traces shown in panel A have been fitted to an exponential function ($F_{obs}=F_0+\{F(t=\infty)-F_0\}\{1-\exp(-k_{obs}\cdot t)\}$). B. The values of k_{obs} have been plotted as a function of the NO concentration. Protein concentration: 20 nM in 100 mM potassium phosphate buffer (pH=6.8). All time traces were measured at room temperature

The sensor described here would be suitable, therefore, for detecting extracellular macrophage derived NO. Other examples relate to monitoring of industrial exhaust gases where NO levels may rise into the micromolar range (E.Hawe 2007) (G.Dooly 2007), the study of the physiological effects of elevated NO levels in mammals (Bowen et al. 2007;Chapman and Wideman 2006), and the study of the equilibrium kinetics of transition metal complexes in which NO is one of the coordinating ligands (Bates et al. 1991;Roncaroli et al. 2003;Strianese et al. 2010a).

Selectivity and Control experiments

The fluorescence intensity of the Atto620 labeled CcP system upon NO binding in the presence of large excesses of NO_2^- , NO_3^- , examples of biologically relevant and potentially competing ions, was checked to obtain an indication on the selectivity of the construct. It is evident from fig. 14 that in the presence of a large excess of NO_2^- or NO_3^- over the protein concentration there is still a clear and large effect on the sample fluorescence when NO is introduced into the solution. NO_2^- causes a slight increase in the fluorescence (see fig. 14). It is known that NO_2^- under acidic conditions is partly converted into NO and the observed increase in fluorescence is ascribed to this effect.

Several research groups have examined the interaction of CcP with small ligands other than NO (e.g., CN^- , F^- , and CO) (Edwards and Poulos 1990) (Yonetani and Anni 1987). Some of the complexes formed upon interaction of CcP with small ligands were found not to be stable; for example the dioxygen adduct of CcP has a half life of 200 ms at 23 °C (Miller et al. 1994). By contrast, NO is one of the most powerful strong field ligands, which occurs on the right end of the spectrochemical series (Jorgensen C.K. 1962; Tsushida R 1938). One may expect, therefore, that the CcP–NO complex will exhibit excellent stability, which is clearly borne out when comparing, for example, the dissociation constant of the CcP- F^- complex (305 μM) (Yonetani and Anni 1987) with that of the CcP–NO complex (10 μM , this project). This suggests that the binding of NO to CcP is strongly preferred over other analytes. This was a further reason to select CcP for implementation in a NO biosensor.

To assess the potential of the NO sensing system in the presence of oxygen, the fluorescence intensity of CcP labeled with Atto 620 was monitored when saturating the buffer with oxygen prior to the measurements. A fast and sizeable increase in the fluorescence intensity upon NO addition is observed (fig. 15). This shows that the rate of NO binding to CcP is fast compared with the rate of

reaction of NO with O₂, and that on the time scale of the measurement O₂ does not interfere with NO detection.

No significant changes in the fluorescence intensities were observed in:

- absence of NO
- free dyes Cy5 or Atto620 labeled BSA
- unlabeled CcP were used as sensing materials

Furthermore when adding 360 μM of nitrate, CO and oxygen, the proposed sensor did not exhibit a change in fluorescence (fig. 16). The lack of an effect of CO and O₂ binding is most likely due to the fact that the CcP we are working with is in the Fe³⁺ state while O₂ and CO have a strong preference for Fe²⁺. Differently, when adding 360 μM of nitrite, the fluorescence intensity of the system slightly increased. As argued above, this is probably due to the NO produced by nitrite (figs. 14, 15 and 16) (Strianese et al. 2010a).

The shelf life of the Ccp_Atto620 biosensor in solution was measured. We added 360 μM of NO (2mM NO saturated buffer) and find that the fluorescence signal decreased in the time, in fact after 7 days the fluorescence tends to zero (fig. 17).

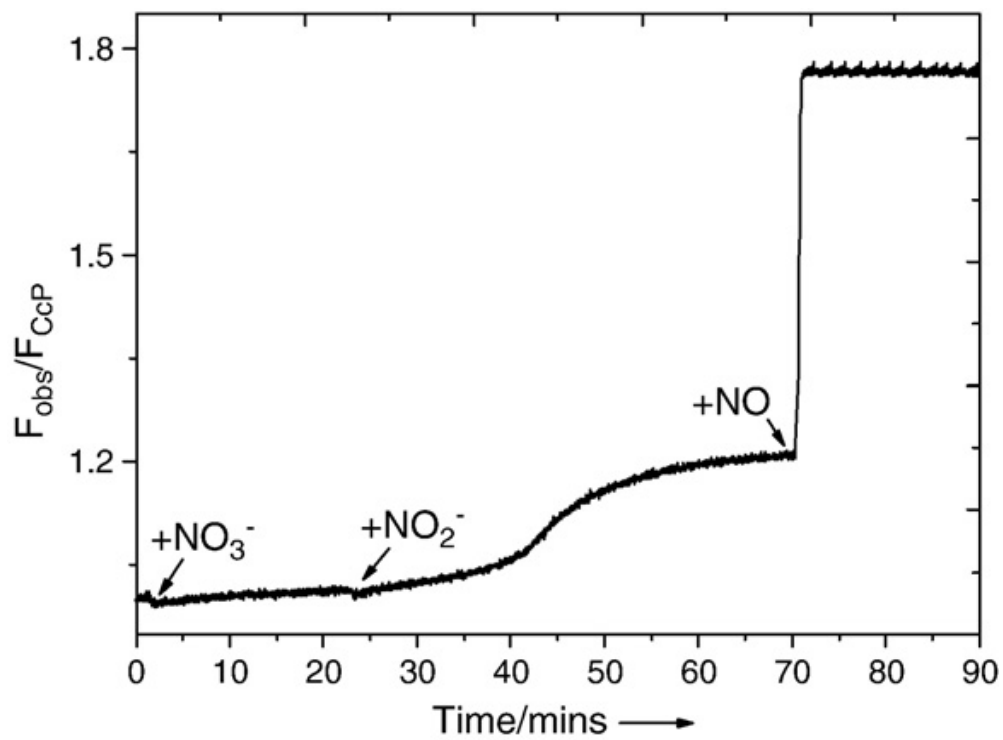


Fig. 14 Fluorescence time trace of Atto620 labeled CcP after subsequent additions of 360 μ M of NO₃⁻, 360 μ M of NO₂⁻ and 360 μ M of NO. Protein concentration: 60 nM in 100 mM potassium phosphate buffer (pH=6.8)

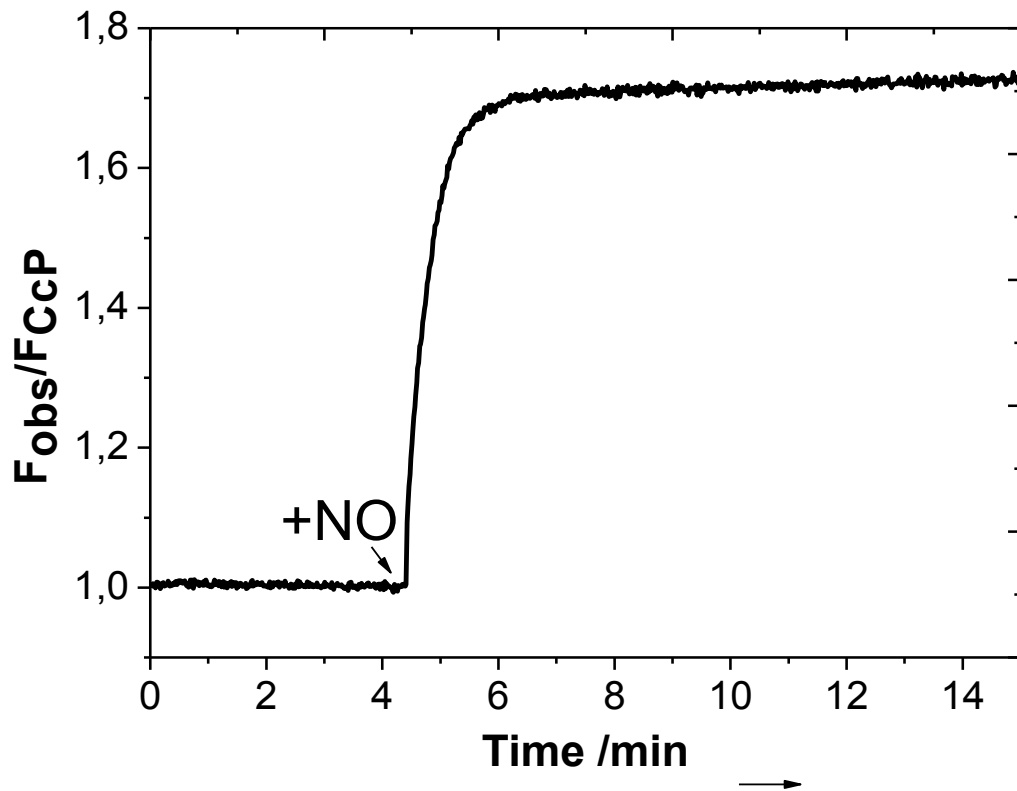


Fig. 15 Fluorescence intensity time trace of CcP/Atto620 upon NO binding in the presence of oxygen. Protein concentration: 70 nM in 100 mM potassium phosphate buffer (pH =6.8); air saturated solution ($[O_2] = 1.3$ mM); $[NO] = 400$ μ M

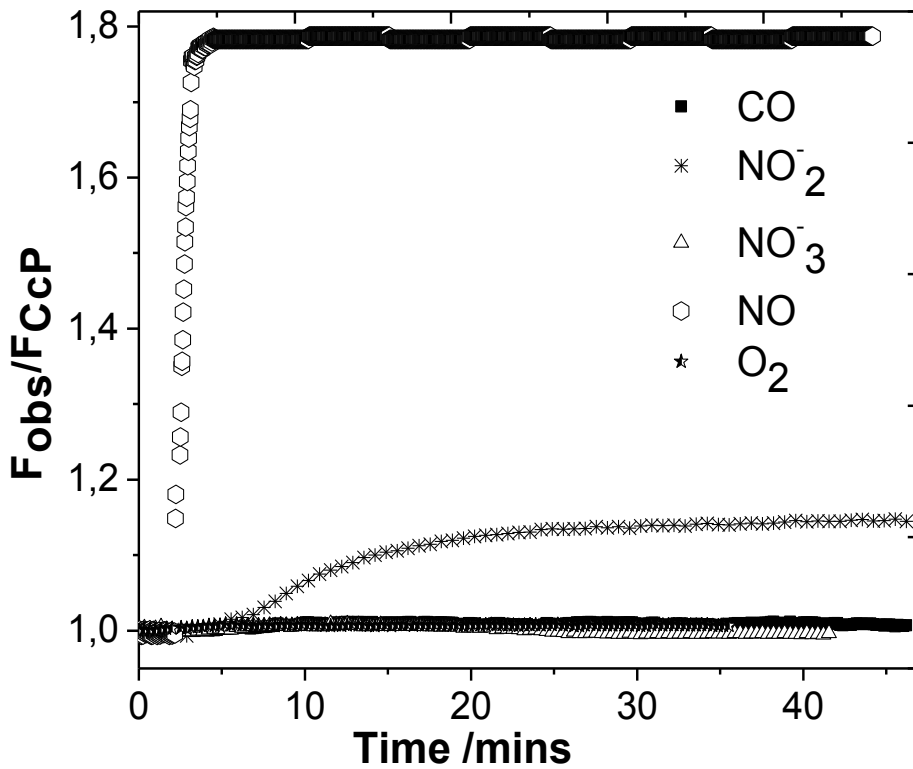


Fig. 16 Fluorescence intensity time traces of Atto620 labeled CcP after additions of 360 μ M of CO , 360 μ M of NO_3^- , 360 μ M of NO_2^- , 360 μ M of NO , 360 μ M of O_2 . Freshly prepared Atto620 labeled CcP was used for each addition experiment. Protein concentration: 80 nM in 100 mM potassium phosphate buffer (pH =6.8). The data points for O_2 are hidden behind those of CO and NO_3^- .

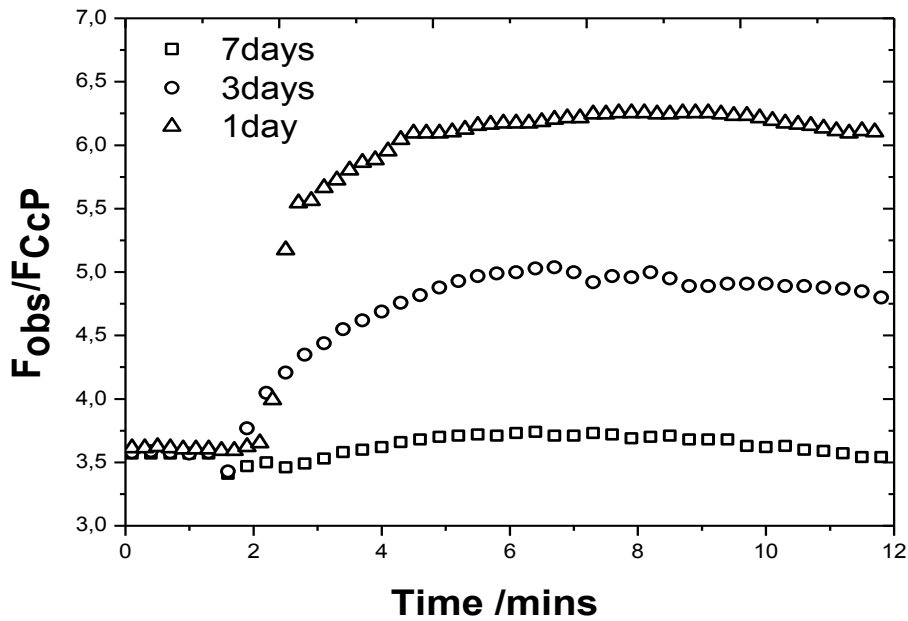


Fig. 17 Shelf life experiment of CcP Atto620 biosensor in 100 mM potassium phosphate buffer (pH =6.8). 360 μ M of NO was added. NO saturated buffer was used (2mM)

Immobilization in Sol Gel matrices

Inorganic gels have been known since the early developments of chemistry, with publications on the synthesis of silica gels from alkoxides in 1846 by Ebelmen M. (Ebelmen M. 1847).

In order to demonstrate the potential of the CcP protein based method for a solid-state NO sensing device, we combined the approach presented with an immobilization technique. This has the potential to provide a more stable and, above all, reusable sensor. Two requirements for an optically biosensor are (a) transparency and (b) inertness of the matrix chosen for the immobilization. These requirements are met by silica based matrices, which, especially in the last decade, have become an established tool for enzyme encapsulation giving rise to biocatalysts that can be easily recycled (Pierre A.C. 2004). By tuning the polymerization reaction conditions (e.g. pH) these so called sol-gel materials can be designed for a given specific application meaning that the gels can be tailored to a range of porous textures, network structures, surface functionalities and processing conditions. Furthermore, the manufacture of the sol-gel does not require harsh reaction conditions which is an advantage when working with the often delicate proteins that have to be incorporated in the matrix. It allows proteins to retain their native structure, spectroscopic properties and (catalytic) activity upon encapsulation into the matrix. The compounds by which the silica network is built around the enzyme are termed precursors. One of the most commonly used compounds is the Alkoxide tetramethoxysilane (TMOS), which is by far the best studied and the most used among a variety of precursors now available (Pierre A.C. 2004; Zauner et al. 2008) .

CcP N-terminally labeled with either Cy5 or Atto620 was entrapped in TMOS and immobilized on a quartz support.

The sol gel solution was quickly poured onto a home made device (8x30 mm² quartz slide Heraeus 3 quality with a 1 mm thickness) yielding a roughly 0.6mm

thick sol-gel layer on top of the quartz slide. Then the fluorescence measures are made in closed cuvette (fig. 18) (see also Materials and methods).

Binding of NO to the immobilized and entrapped CcP was found to be reversible: insertion of the construct into an NO containing solution resulted in a fluorescence increase. Subsequent bubbling of argon through the solution removed the NO again (fig. 19). Labeled CcP immobilized into a TMOS matrix kept its activity in terms of SR and time response for more than 20 days when stored at 4 °C. The SRs observed were lower than the ones obtained in the solution measurements (e.g., in the case of 360 μ M NO an SR of 20% was found with Cy5-labeled CcP when measuring the sol-gel sample, while 40 \pm 5% was found in the bulk experiment). These findings may be related to a fraction of encapsulated protein not being accessible to the substrate or having been damaged and having lost its capability to bind NO. The fluorescence time traces could be fitted to the same exponential function as used for the solution experiments (see Eq. (4)).

Not surprisingly, the rates of NO binding were smaller, most likely due to the time needed for the NO to diffuse into the TMOS matrix. A similar behaviour was found for immobilized hemocyanin when it was used to monitor oxygen concentrations (Zauner et al. 2008).

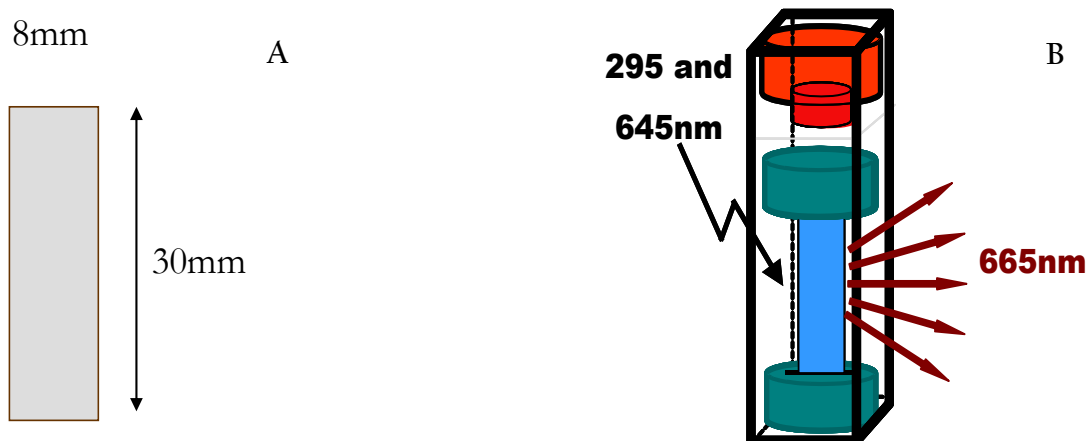


Fig. 18 The device to measure the sol gel samples. A) quartz slide. B) quartz slide in the fluorescence cuvette

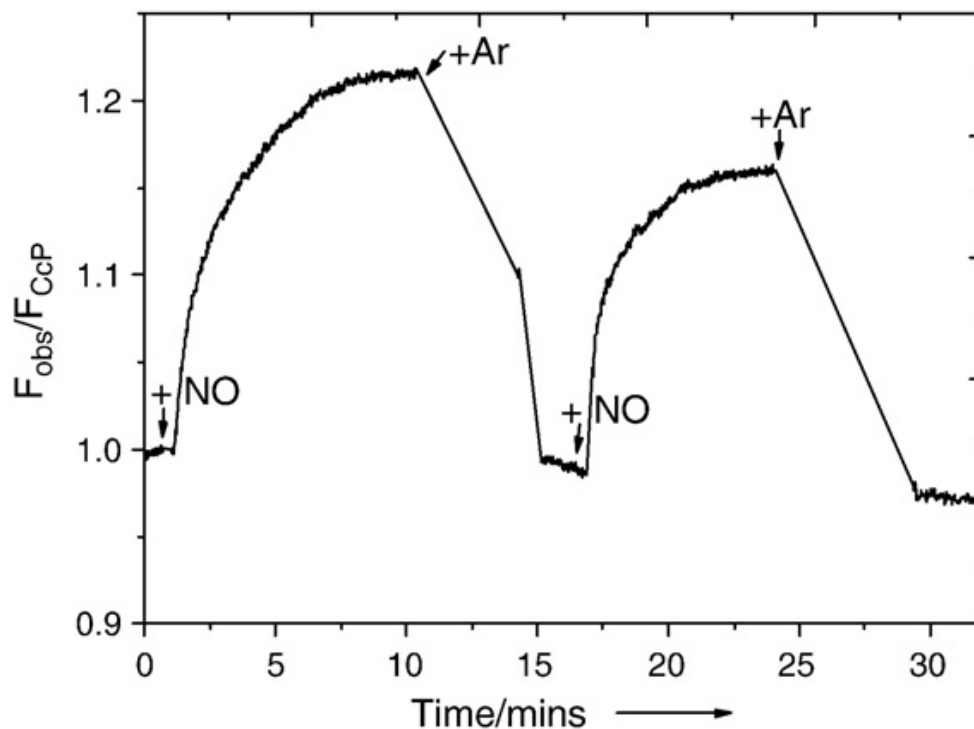


Fig. 19 Fluorescence intensity time trace at 665 nm (exc 645 nm) of Cy5-labeled CcP entrapped into a TMOS-based sol-gel immobilized on a quartz support upon addition and removal of NO. During the measurement the sensing device was placed in 100 mM potassium phosphate buffer (pH=6.8) at room temperature. The fluorescence was recorded while alternatingly NO was added (to a final concentration of 360 μ M) to the solution and removed by refreshing the buffer and bubbling argon through the solution

The shelf life of the sol gel device was measured. In this case we used CcP labeled with Cy5. We find that the fluorescence signal decreased in the time, in fact after 14 days we measured a signal loss of 75% with a S.R. which tends to background signals (fig. 20).

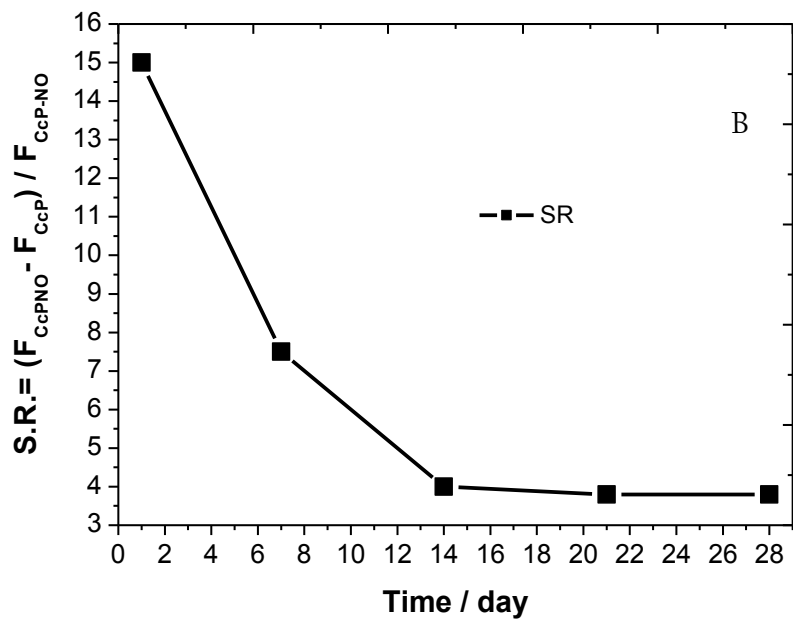
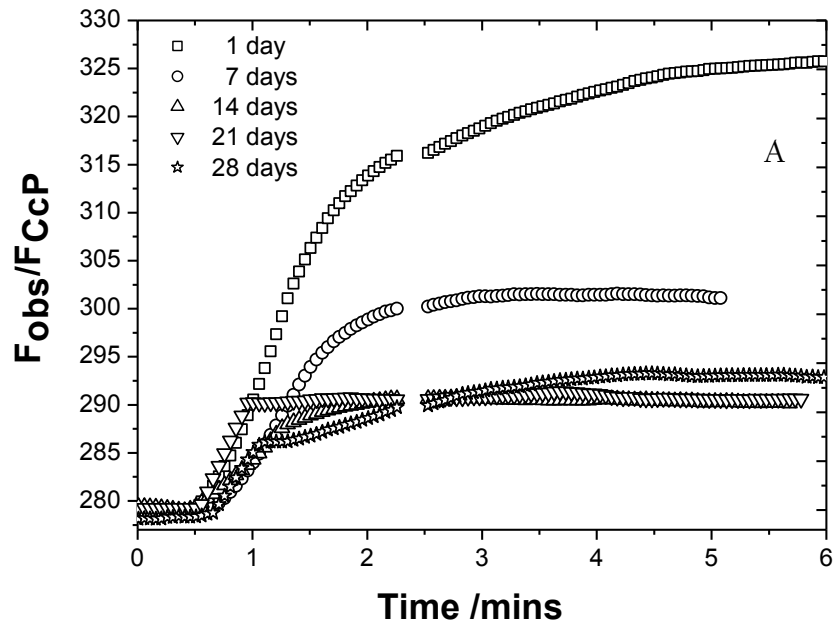


Fig. 20 A) Fluorescence measured of the sol gel with Ccp_Cy5 biosensor. NO saturated buffer used (2mM).
 B) Switching ratio of the same experiment calculated in 4 weeks

Application of the CcP_Atto620 NO Biosensor in *Arabidopsis thaliana* suspension cell culture

Heavy metal stress and monitoring of the NO production

In (De Michele et al. 2009), Prof. Lo Schiavo and his groups was showed that *Arabidopsis* (*Arabidopsis thaliana*) cell suspension cultures underwent a process of programmed cell death when exposed to 100 and 150 mM CdCl₂ and that this process resembled an accelerated senescence, as suggested by the expression of the marker senescence-associated gene12 (SAG12). CdCl₂ treatment was accompanied by a rapid increase in nitric oxide (NO) and phytochelatin synthesis, which continued to be high as long as the cells remained viable. Hydrogen peroxide production was a later event and preceded the rise of cell death by about 24 h. Furthermore, they found NO maximum production after 24h to start the treatment. However, in this case they have used DAF-2 to measure the NO (indirect measure) and check the NO production in the time.

In order to simulate this process, of course, we tried to design a similar experiment as describe by (De Michele et al. 2009), using a CcP-Atto620 biosensor instead of DAF-2, but with a fundamental difference in the design of the experiment. In fact, a Ccp-Atto620 biosensor measure directly NO extracellular concentration, therefore making it necessary to minimize or completely eliminate the O₂ in the sample. Naturally, all the components and solutions were degassed with Argon, with the *Arabidopsis* cell suspension being inserted into closed glass vials in order to avoid or minimize O₂ atmospheric contact.

The *Arabidopsis* cell suspension cultures were treated with 50, 100, and 150 µM CdCl₂, with their growth and viability being measured at different times after

treatment. The fresh weight of the cells grown with 50 μM CdCl_2 did not differ from that of the untreated cells at any time during the analysis. Cell cultures of *Arabidopsis* were chosen as an experimental system because the homogeneity and undifferentiated state of the cells, combined with the uniform delivery of the treatments, allow for a clear and reproducible response. The cell culture was transferred to a new AT3-medium weekly. We used three day old cell suspensions.

In order to verify the process, we prepared two parallel experiments under the same conditions but using the two different optical biosensors. Then we monitored over time the NO production in *Arabidopsis thaliana* cells suspensions. The first biosensor was Ccp_Atto620, developed in our laboratory, while the second is DAF-2 in reference to the method used in (De Michele et al. 2009). Both experiments were carried out under the same conditions.

The monitoring of the NO production is reported in the figs. 21 and 22. The difference of NO production, measured with DAF-2 (fig. 21) and Ccp_Atto620 (fig.22) is reported, with the different meaning between indirect and direct measurements of NO in fluorescence being shown.

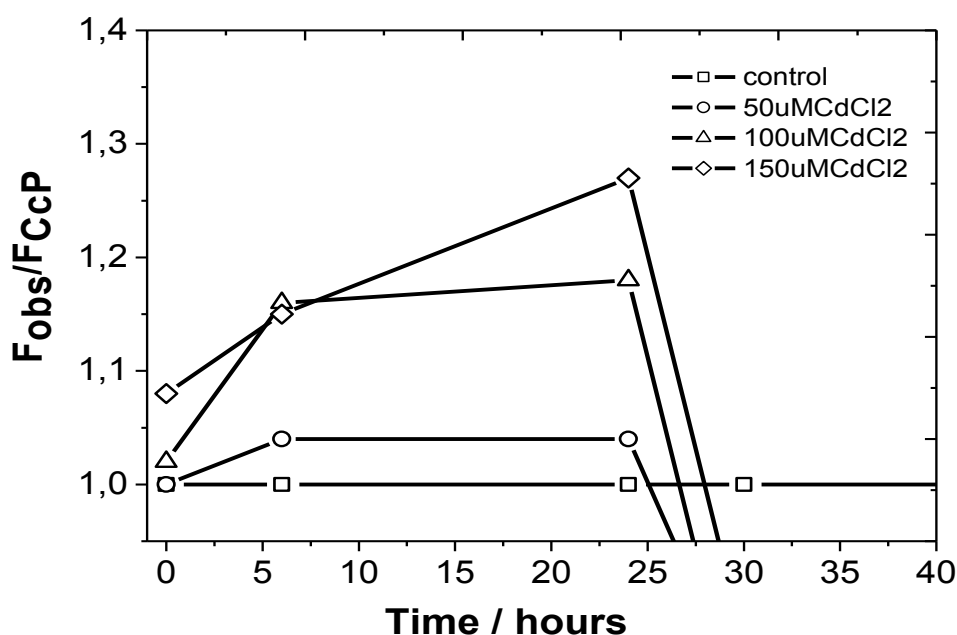


Fig. 21 NO in *Arabidopsis* suspended cells measured with DAF-2. On the Y axis we reported the ratio between fluorescence of the sample and the controls (without CdCl_2) and on the X axis there is the time expressed in hours.

The first result of this experiment with DAF-2 (fig. 21) reports the same results obtained from (De Michele et al. 2009). In fact, after 24h there is a maximum presence of NO at a maximum concentration of CdCl₂.

With DAF-2, we carried out an indirect measurement. After 24h, there is a reduction of fluorescence which is probably caused by the rapid death of the cells due to the harsh conditions the cells were submitted to. This result means that we measured an accumulation of the oxidation product of NO in the extracellular environment.

Upon using the CcP_Atto620 biosensor we obtained similar results (fig 22).

In fact at 24h, the maximum signal of the fluorescence at 150 µM of CdCl₂ and after a rapid reduction of signal was observed. However, in this case a direct measurement of the NO present in the solution was obtained and not an indirect measured as in the case of DAF-2.

In this case we measured the NO production in that moment. At 24h also the signal of 50 and 100 µM CdCl₂ was also consistent with the expected result as well as in DAF-2 (De Michele et al. 2009).

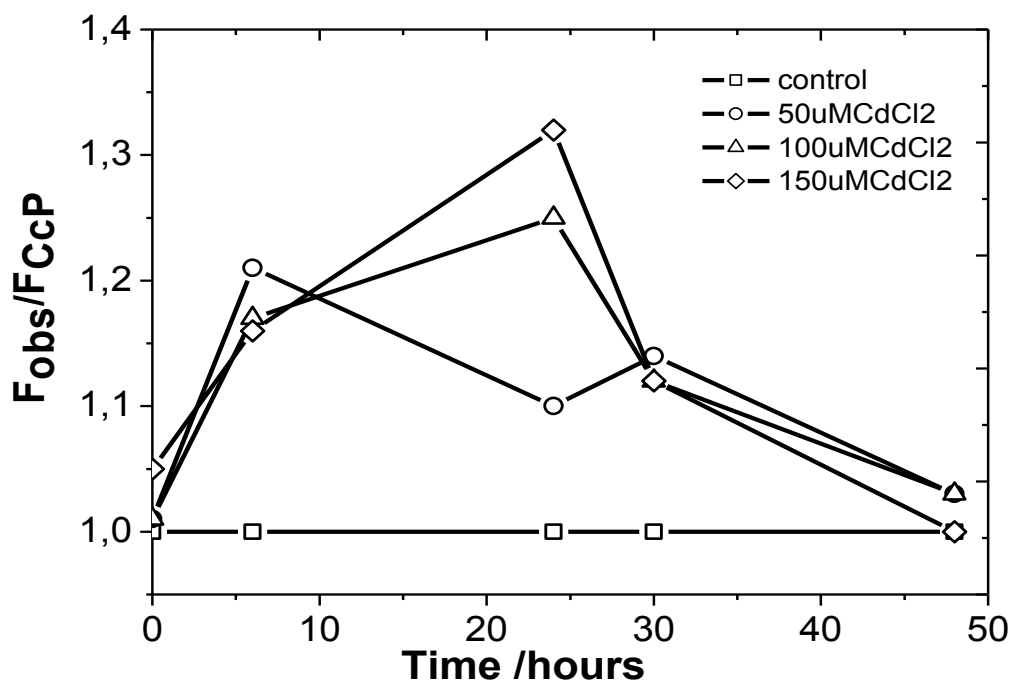


Fig. 22 NO in Arabidopsis suspended cells measured with CcP_Atto620. On the Y axis we reported the ratio between the fluorescence of the sample and the controls (without CdCl₂) and on the X axis there is the time expressed in hours.

This confirms that it is possible to use the Ccp_Atto620 biosensor *in vivo* with suspension cell culture and that the results for qualitative analysis are similar to another fluorescence method (DAF-2) used with standard methods.

In Ccp_Atto620 we used Cytochrome c' peroxidase as a biological component. It is a protein that has the function of taking reduced equivalents from cytochrome c and reduces hydrogen peroxide to water. In (De Michele et al. 2009), in addition to NO measurements, H₂O₂ was also considered. However, the measurements of H₂O₂ released in the culture medium revealed undetectable levels in untreated cells and in cells treated for up to 3 d with 50 µM CdCl₂.

At the higher concentrations, we observed a dose dependence with the CdCl₂ initiation and an intensity of H₂O₂ production. Treatment with 100 µM CdCl₂ resulted in an increase in H₂O₂ content at 72 h after treatment. At a concentration of 150 µM CdCl₂, H₂O₂ levels increased at just 48 h after treatment and remained high the following day (De Michele et al. 2009). In this case they found the maximum amount of H₂O₂ after 48 h from the beginning of the experiment for a maximum of 0,8 µmol/gFW (De Michele et al. 2009) while at 24h they noticed values near zero.

Therefore we have considered the amount of H₂O₂ measured in the extracellular environment in 2009 (De Michele et al. 2009) and verified the tolerant CcP amount making a titration with H₂O₂ verifying the difference in UV-Vis spectra. In fact if no modification in the UV spectra under 0,8 µmol/gFW was showed the CcP isn't "annoyed" to H₂O₂ present in extracellular environment.

In fig. 23 we report that at least 350nM of H₂O₂ is required to modify CcP UV spectra (α and β bands, respectively 535 and 560 nm) and then the fluorescence system when the protein is labelled. However, we assume a lower amount of H₂O₂ within 24h. All the experiments were repeated at least twice.

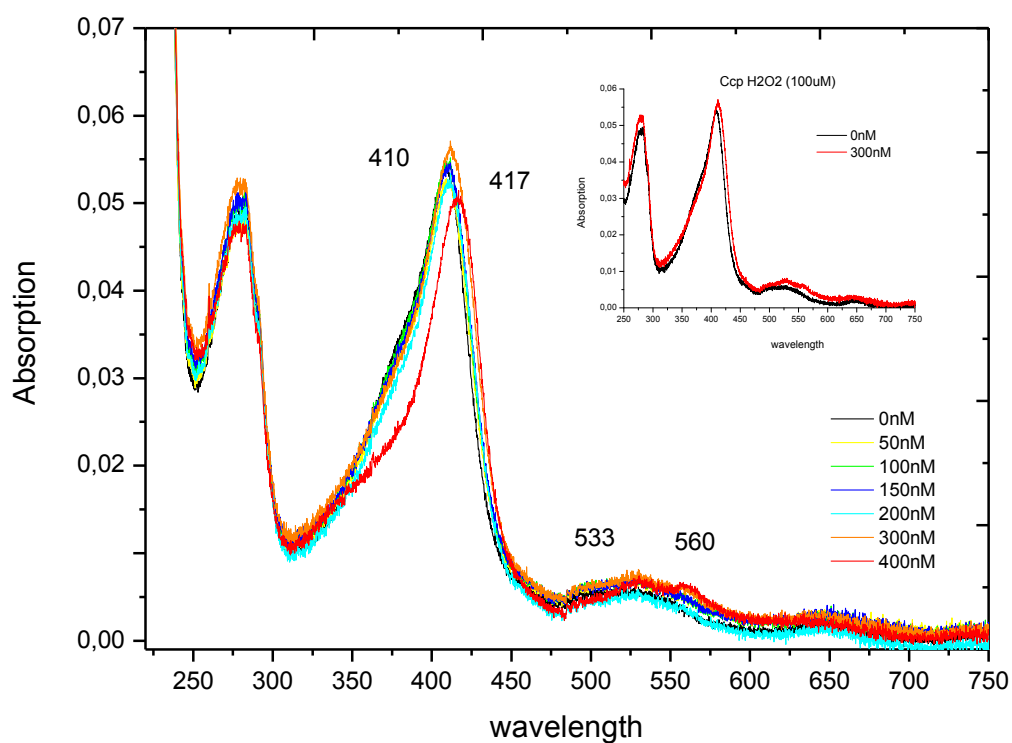


Fig. 23. Titration of Ccp with H₂O₂ 100µM. We verified the coordination of the H₂O₂ to CcP. We considered the change of Soret, α and β bands.

Internal Cd²⁺ quantification

In order to confirm whether Cd²⁺ ions were able to enter the cells, we measured their internal concentration through atomic absorption spectrometry. The amount of Cd²⁺ inside the cells was correlated to the treatment dose. Sampled cells treated with 50 mM CdCl₂ after 48h contained 0,194 nmol mg⁻¹ dry weight Cd²⁺, whereas treatments with concentrations of 100 and 150 mM resulted in 5.21 nmol mg⁻¹ dry weight and 6.15 nmol mg⁻¹ dry weight internal Cd²⁺, respectively. The cells were treated as described in Materials and Methods.

NO Quantification in Arabidopsis thaliana suspension cell culture

The detection and direct measurement of NO were defined. The next step was to quantify the NO present in the sample. Under the same conditions as before we prepared a calibration curve with MAHMA NONoates in order to quantify NO in Arabidopsis suspension cell culture (fig. 24). We prepared four standard curves 20, 40, 80 and 160uM of NO. It is worth recalling that the molecular ratio of MAHMA NONoates vs NO is 1:2. All the preparation steps for the standard were carried out in dry ice in order to avoid NO release. The calibration curves were built using a S.R. index $((F_{\text{CCP-NO}} - F_{\text{CCP}}) / F_{\text{CCP-NO}})$ and the parameters obtained were $R = 0,985$ and $SD \pm 2,63$.

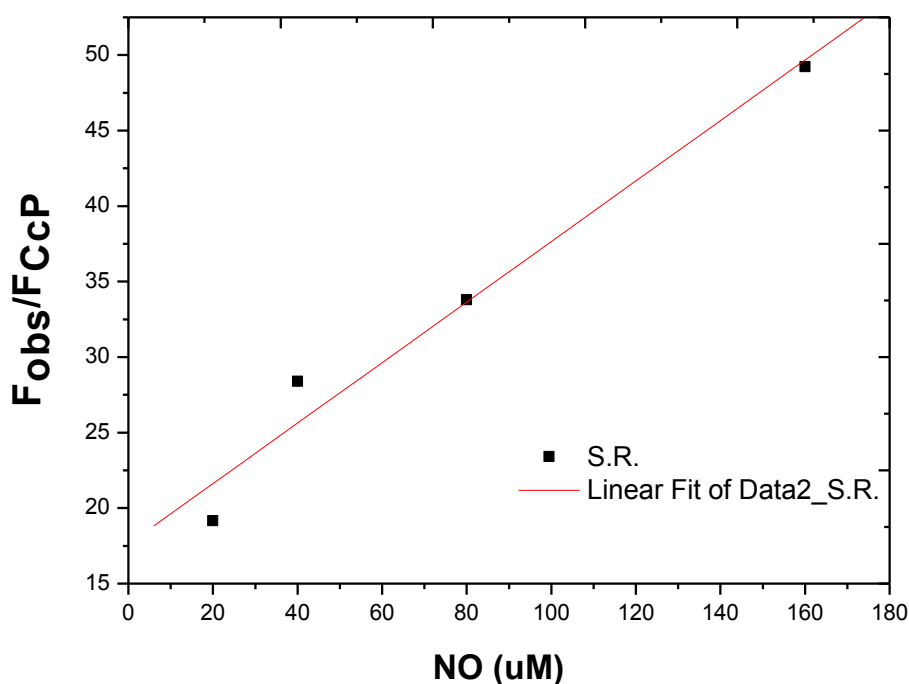


Fig. 24 Standard calibration curve prepared with Mahma NONOate

The nitric oxide extracellular theoretical values were obtained at different CdCl₂ concentrations. In the Arabidopsis suspension cell culture were:

$$50\mu\text{M CdCl}_2 = 9,11 \mu\text{M}$$

$$100\mu\text{M CdCl}_2 = 20,78 \mu\text{M}$$

$$150\mu\text{M CdCl}_2 = 25,49 \mu\text{M}$$

There are no similar results in current literature. However, these results are in agreement with the quantity of Cd²⁺ used to stress the cells and respects the proportion between concentrated used in each sample and their response.

Myoglobin: Hydrogen sulphide biosensor

Absorption spectra and F.R.E.T. system

The H₂S binding to the Fe of Mb is a commonly accepted finding. Several research groups have studied the mechanistic details of the binding of this molecule to Mb (Berzofsky Jay A. et al. 1971; Berzofsky Jay A. et al. 1972; Nicholls P. 1961). We extended the same approach to myoglobin from horse skeletal muscle (Mb) to design a H₂S sensor, along the FRET principles. Spectroscopic features of Mb make it ideally suited for implementing a FRET based H₂S biosensor. Specifically, while the absorption spectrum of Mb exhibits a characteristic Soret band at 409 nm and two less intense bands centered respectively at 503 nm and 636 nm, H₂S addition shifts the Soret band at 421 nm, quenches the 503 and 636 nm bands and leads to the appearance of three new bands at 543 nm, 581 nm and 617 nm (Nicholls P. 1961) (Strianese et al. 2010b)(see fig 25). This change of the absorption spectrum of Mb will strongly modulate the fluorescence properties of a FRET donor acceptor pair, with the Fe site as the energy acceptor and a dye label, as the fluorescent donor.

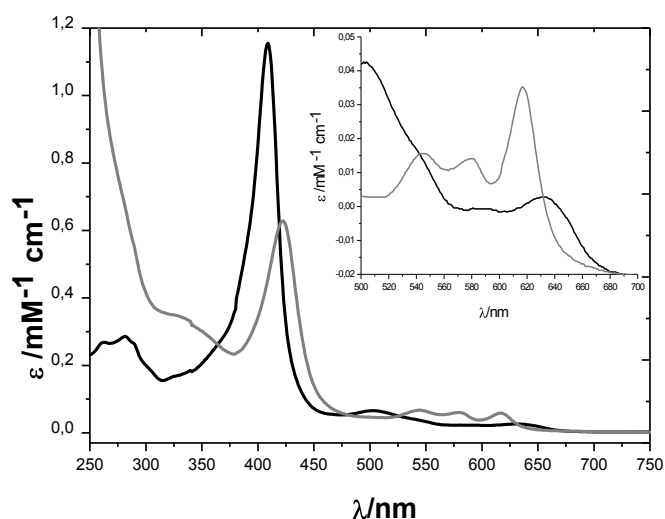


Fig. 25 Absorption spectrum of H₂S -free (black) and H₂S-bound (grey) Mb. Inset: 500-800 nm region of the spectrum with enlarged vertical scale of the H₂S-free Mb (black) and of the H₂S bound form (grey).

The idea is that using a dye label emitting in the 550-570 nm range when the protein in the H₂S -free state, the fluorescence of the dye is essentially uninhibited, whereas as soon as H₂S binds to Mb, the fluorescence of the label is quenched as a result of energy transfer to either the 543nm or the 581 nm band (depending on the emission of the dye label chosen for labeling Mb). That is to say that the H₂S binding to labeled Mb “turns off” the dye fluorescence. Differently, using a dye label emitting around 640 nm when the protein in the H₂S -free state, the fluorescence of the dye is initially quenched as a consequence of energy transfer to the 636 nm band, whereas as soon as H₂S binds to Mb, the 636 nm band disappears and all the energy absorbed by the label is emitted as fluorescence. In this case we have a “turn on” biosensor (Strianese et al. 2010b). It follows that the fluorescent label acts as a sensitive reporter of the H₂S bound to the iron center. Two different fluorescence probes, Cy3 and Atto620, were selected for this study. The overlap of the Mb absorption bands (H₂S -free and H₂S -bound forms) with the emission spectrum of either Cy3 or Atto620 can be judged from fig. 26

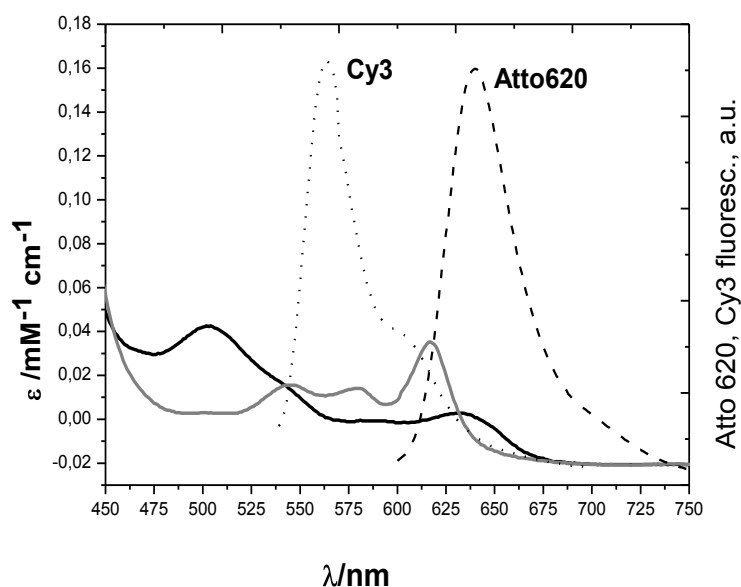


Fig. 26 Absorption spectrum of H₂S-free Mb (dark line) and of the H₂S -bound form (grey) and emission spectra of Cy3 ($\lambda_{\text{max}} = 570$ nm) and of Atto620 ($\lambda_{\text{max}} = 645$ nm). All spectra measured at room temperature. Protein concentration: 9 μM in 100 mM potassium phosphate buffer (pH =6.8).

The optical characterization of the Mb- H₂S adduct has been already reported (Berzofsky Jay A. et al. 1971; Berzofsky Jay A. et al. 1972; Nicholls P. 1961).

In our experiments Mb was covalently labeled either with Cy3 or with Atto620. To test the system, the fluorescence intensity of labeled Mb was monitored as a function of time during a change from an H₂S -saturated to an H₂S -free environment. Fig. 27 shows a typical time trace of a solution containing 100 nM of dye-labeled Mb when excited at the absorption maximum ($\lambda = 550$ nm) of the dye (Cy3) (Strianese et al. 2010b). In this particular experiment each cycle was started by adding H₂S to an end concentration of 50 mM (i.e., in excess over the Mb concentration) and completed by passing argon through the solution for the complete removal of H₂S. The dye emission was followed at 570 nm.

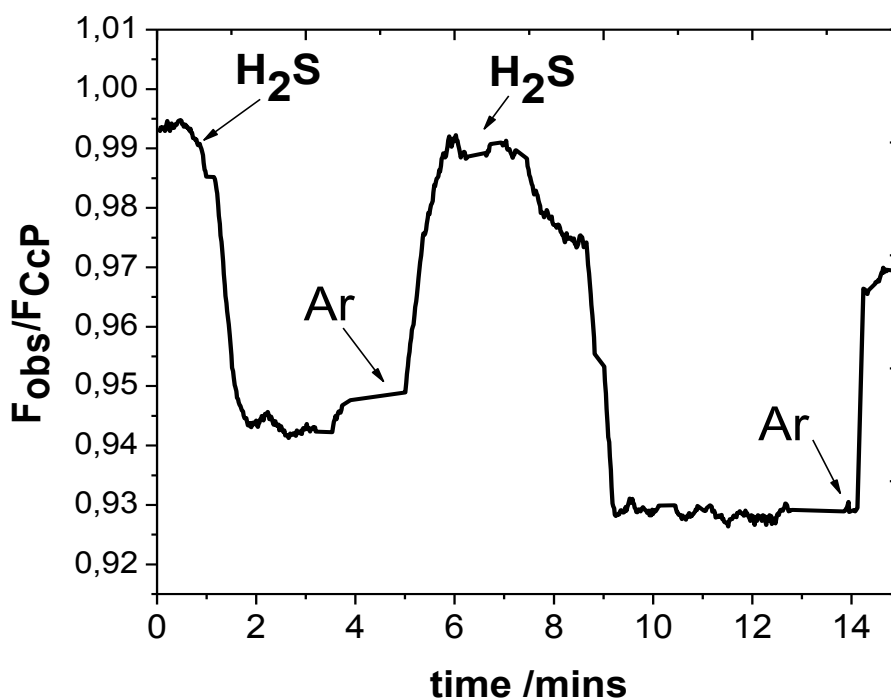


Fig. 27 Room temperature fluorescence intensity time trace observed at 570 nm (exc 550 nm) of Cy3 labeled Mb, upon addition and removal of H₂S. Protein concentration: 100 nM in 100 mM potassium phosphate buffer (pH =6.8). In this particular experiment a standard solution of (NH₄)₂S was used as H₂S source. The H₂S content of the (NH₄)₂S standard solution was quoted by a coulombometric

A fluorescence quenching of label emission was clearly observed upon each H₂S addition. When bubbling argon through the sample solution to displace the H₂S, the initial fluorescence intensity of the label was restored; the cycle could be repeated many times. This finding showed that, in the experimental conditions tested, the H₂S binding process is reversible, which is crucial for practical sensing applications.

When monitoring the Atto620 labeled Mb sensing construct under the same conditions, an opposite trend was observed (fig 28)(Strianese et al. 2010b). An increase in label emission was observed upon each H₂S addition. When displacing the H₂S by bubbling through argon, the fluorescence intensity of the label diminished again. Despite the relatively low amplitude observed for the fluorescence signals, the different trend observed for the two sensing constructs tested (which perfectly matches the fact that when labeling Mb with either Cy3 or Atto620 we are looking at different absorption bands of Mb), indicates that our method is sensitive enough.

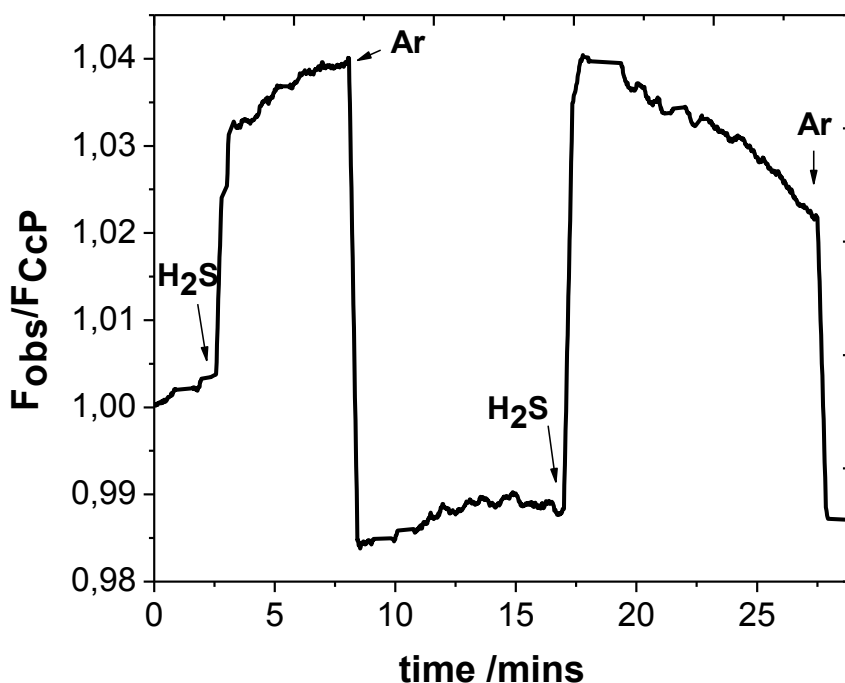


Fig. 28 Room temperature fluorescence intensity time trace observed at 645 nm (exc 620 nm) of Atto620 labeled Mb, upon addition and removal of H₂S. Protein concentration: 120 nM in 100 mM potassium phosphate buffer (pH =6.8). In this particular experiment a standard solution of (NH₄)₂S was used as H₂S source. The H₂S content of the (NH₄)₂S standard solution was quoted by a coulombometric titration experiment

Very interestingly the proposed sensor is highly selective for the detection of hydrogen sulphide against other thiols like cysteine or glutathione (GSH). Contrary to the clean changes in the UV-Vis and fluorescence spectra of unlabeled and labeled Mb observed upon addition of hydrogen sulphide, the addition of a large excess of either cysteine or GSH did not result into significant changes in the UV-Vis spectrum and in the fluorescence intensities of the system (figs. 29, 30)(Strianese et al. 2010b).

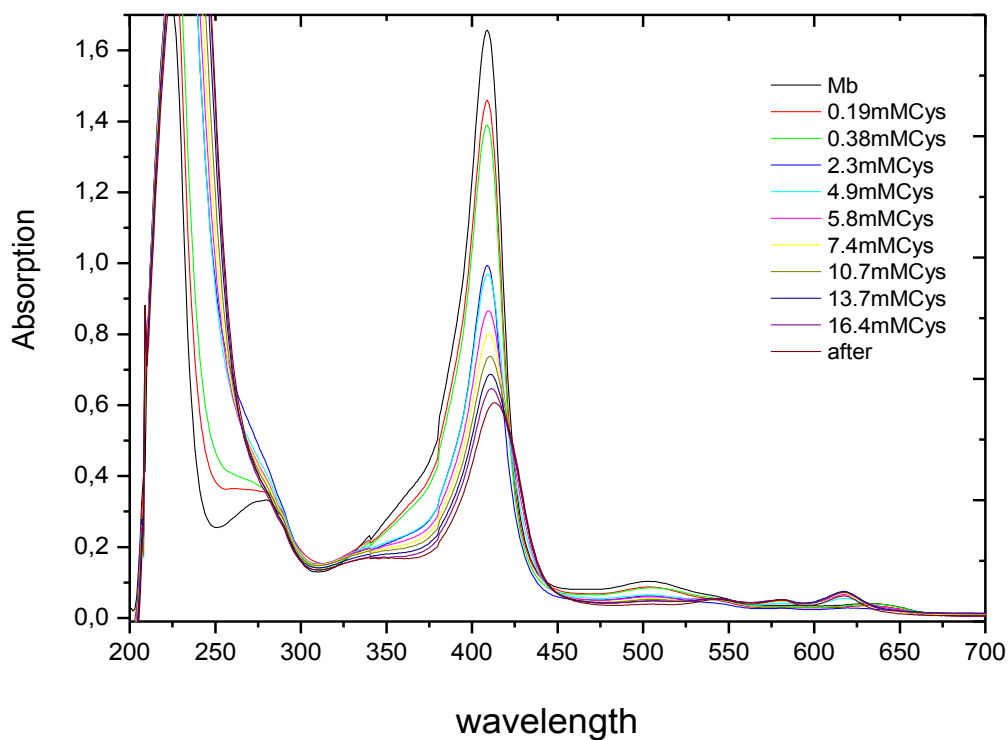


Fig. 29 Titration of Mb with L-Cysteine (100mM)

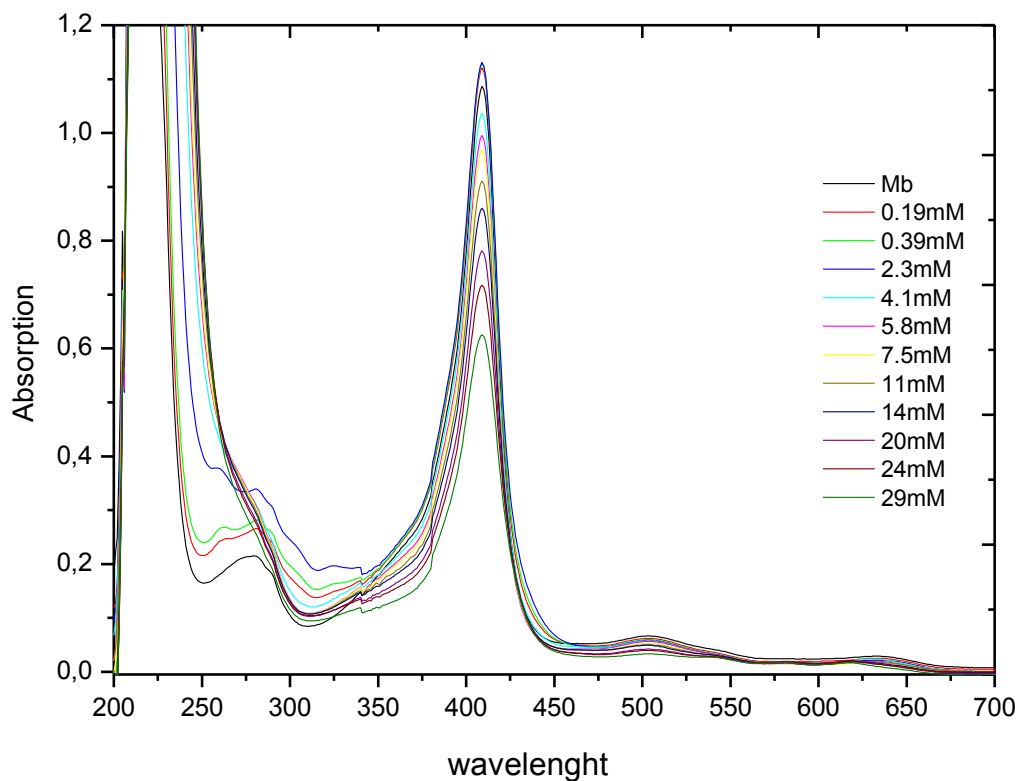


Fig. 30 Titration of Mb with L- Glutathione (100mM)

Immobilization into sol gel matrices

In order to demonstrate the potential of this Mb based method for a solid-state H₂S sensing device, we combined our approach with an immobilization technique. As well as Ccp also the Mb labeled with either Cy3 or Atto620 was entrapped in a silica (TMOS) matrix and immobilized on a quartz support as described in “Materials and Methods, Chapter four”. Binding of H₂S to the immobilized and entrapped Mb was found to be reversible: insertion of the

Mb/Atto620 construct into an H₂S containing solution resulted in a fluorescence increase. The bubbling of argon through the solution surrounding the sample drove the removal of H₂S to completion (fig. 31)(Strianese et al. 2010b). The immobilization of the sensing device has the potential to provide a more stable and, above all, reusable sensor.

Unfortunately in our investigations the condition of the reusability could not be met. After the first complete cycle of H₂S addition/removal (see fig. 31) when keeping on adding H₂S to the system, the fluorescence intensity was not affected. Most likely the lack of an effect after the first cycle of the experiment could be due to partial denaturation of the encapsulated Mb and consequent loss of its capability to bind H₂S(Strianese et al. 2010b). No significant changes in the fluorescence intensities were observed in the absence of H₂S or when free dyes, Cy3 or Atto620 labeled BSA, or unlabeled Mb were used as sensing material controls(Strianese et al. 2010b).

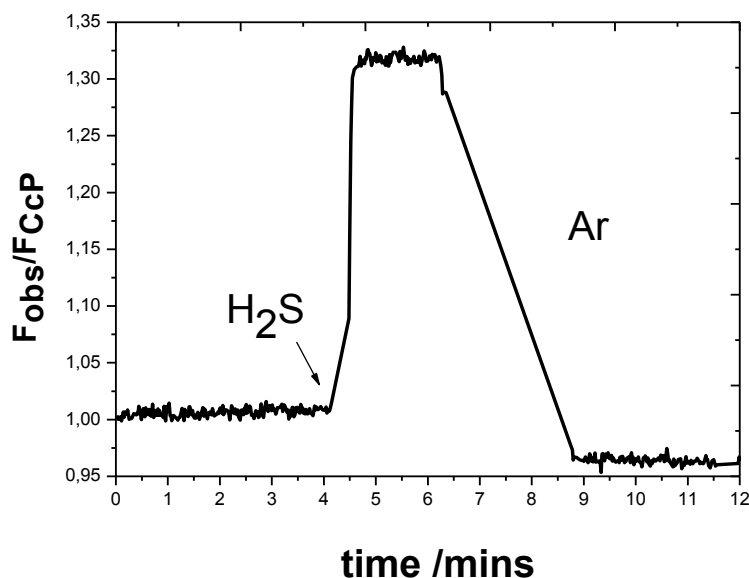


Fig. 31. Fluorescence intensity time trace at 645 nm (exc 620 nm) of Atto620-labeled Mb entrapped into a TMOS-based sol-gel immobilized on a quartz support upon addition and removal of H₂S. During the measurement the sensing device was placed in 100 mM potassium phosphate buffer (pH =6.8) at room temperature. The fluorescence was recorded while alternately H₂S was added (to a final concentration of 50 MM) to the solution and removed by refreshing the buffer and bubbling argon through the solution.

Chapter three - Conclusions

CcP_Atto620. The Nitric oxide biosensor

Fluorescently labeled CcP can be successfully used as a 'turn on' (Lim and Lippard 2007) FRET-based biosensor for NO. Its flexible mode of operation not only in solution but also when applied in the form of a solid state device, makes a CcP-based device suitable for sensing applications. The binding affinity constant (K_d) for the NO binding to CcP was determined to be $10 \pm 1.5 \mu\text{M}$. The rate of NO dissociation from the CcP (k_{off}) and the second order rate constant for the NO association (k_{on}) were found to be $0.22 \pm 0.08 \text{ min}^{-1}$ and $0.024 \pm 0.002 \mu\text{M}^{-1} \text{ min}^{-1}$ respectively. A limitation is that the maximum and minimum fluorescence levels decrease with the number of cycles in a single experiment. It was observed that the maximum and minimum fluorescence levels slowly decrease with the number of cycles the sample solution had gone through. We hypothesize that this could be due to partial denaturation of the CcP after bubbling argon through the solution to displace the NO, because only after bubbling Ar we noticed decrease in the fluorescence levels. In fact the fluorescence intensity of the construct after adding NO remained constant for hours when the solution was left standing.

Possible competitors of the NO were monitored, for example NO_2 , NO_3 , CO and O_2 . While NO_2 added to a Ccp_Atto620 biosensor showed a minimal increase of fluorescence, with no effect being evident when adding CO or O_2 to the CcP. The lack of an effect of CO and O_2 binding is most likely due to the fact that the CcP we are working with is in the Fe^{3+} state while O_2 and CO have a strong

preference for Fe^{2+} . In fact the linear geometry of the Fe^{3+} -NO bond is in favour in contrast to Fe^{2+} .

Our NO sensing system is based on the appearance of a fluorescence signal upon NO binding different from the already existing protein-based methods for NO detection (Barker et al. 1998; Barker et al. 1999a; Barker and Kopelman 1998). In fact this device, using FRET mechanism, directly measures concentrated NO. Although concentration-dependent quenching mechanisms have shown to be successful, (Barker et al. 1998; Zauner et al. 2007) they are inherently less sensitive than methods exploiting fluorescence enhancement or “turn on” as a result of binding (Lim and Lippard 2004; Lim and Lippard 2007; White et al. 2008). Moreover, it is often difficult to distinguish analyte responses from sensor degradation when quenching is relied upon for quantitation (White et al. 2008). The successful immobilization of labeled CcP into a polymeric matrix to provide a solid state NO sensing device presents an advantage in terms of reusability and stability of the system. In this case the SR is lower than in solutions, while the decrease of fluorescence levels is greater than in solution. The protocol of the biosensor is fast and not difficult to prepare.

This device has been proven to be a good tool to measure NO due to it being easier to use and more selective than each other devices present in current literature.

The device has been demonstrated to be a quasi-quantitative system, with the possibility to re-use the same biosensor more times, thus making it a good candidate for the direct *in vitro* and *in vivo* measurement of NO.

CcP_Atto620 NO Biosensor in *Arabidopsis thaliana* suspension cell culture

In the first stage of this work, the protocols and tools to permit the measurement of NO without O₂ extracellular were set up and optimized. The process included a condition and cell growth curve, volume and air medium ratio in flask and in cuvette, as well as the ratio between the device and suspended cells in cuvette.

Bubbling Argon was required for each component and tool used. It is possible that not all the O₂ was removed. However, we obtained the same results using two different device to measured the NO concentrations. In addition, we confirmed the data obtained in (De Michele et al. 2009). In fact they claim that under heavy metal stress *Arabidopsis thaliana* cells produce maximum NO quantity after 24h. With DAF-2A we have confirmed the high level of N₂O₃ present in the extracellular environment, while the Ccp_Atto620 biosensor show the maximum NO production within 24 hours in the liquid culture of *Arabidopsis* (extracellular environment) and later a rapid decrease.

In the suspension cell culture of *Arabidopsis thaliana* stressed with high concentration of Cd²⁺ (150µM) we observed a greater NO production than in suspended cells treated with low Cd²⁺ concentration (100 and 50 µM) within 24h.

At each concentration, we observed a dose-dependence between the measured NO production and amount of CdCl₂ used. In (De Michele et al. 2009) about 2 days after the treatment with 150 µM CdCl₂, the NO level was high. In our case we show that after 24h NO production decreased. This is possible because our experimental conditions are slightly different from (De Michele et al. 2009) and N₂O₃ accumulation levels were not considered in direct measurement of NO.

A possible interference problem could be due to H₂O₂. In fact, a rapid production of H₂O₂ was also reported for Arabidopsis cell cultures treated with 10 to 75 mM Cd²⁺ (Horemans et al. 2007). However, this study did not focus on Cd²⁺ cytotoxicity and its signaling events. We have shown that concentrations up to 50 mM are ineffective at inducing cell death. In our system, we observed an increase in the extracellular H₂O₂ levels only when cultures were exposed to CdCl₂ concentrations inducing PCD (100 and 150 μM)(De Michele et al. 2009). At both doses, the increase in H₂O₂ levels was a late event and preceded cell death by about 24 h (De Michele et al. 2009) and the amount of H₂O₂ was revealed to be very low. In fact, in the same experiment (De Michele et al. 2009) a concentration of 0,8 μmol/gFW of H₂O₂ after 48h was noted.

However, in our experiments after 24h cell death and NO production decrease already begin.

Furthermore, in results section we have highlighted a titration in Uv-Vis with H₂O₂. In this case the H₂O₂ reacts with the CcP after a concentration of 350 nM. Therefore we can consider this amount lower than the one in (De Michele et al. 2009).

This is currently the first example of the direct measurement of the extracellular production of NO *in vivo* and no other similar experiments are present in current literature.

Myoglobin as a hydrogen sulphide biosensor

The data provided proof-of-principle that fluorescently labeled Mb can be used as a FRET based biosensor for H₂S. Its flexible mode of operation not only in solutions but also when in the form of a solid state device, makes a Mb-based device suitable for sensing applications. A limitation is that by subsequent additions of H₂S, ferric sulph-Mb is reduced to the ferrous form (Berzofsky Jay A. et al. 1972). The latter complex is extremely stable and under these experimental conditions the H₂S binding becomes irreversible. This makes it difficult to calculate a dissociation constant (Strianese et al. 2010b).

The possibility of turning “on” or “off” the fluorescence of labeled Mb upon H₂S binding by simply changing the dye molecule to label Mb offers versatility to our system and make it adaptable to the specific needs of a given experiment.

The device in a solid state can be used as “one-pot” biosensor because is not possible to completely remove the H₂S after addition. Moreover the successful immobilization of labeled Mb into a polymeric matrix to provide a solid state H₂S sensing device presents an advantage in terms of stability of the system (Strianese et al. 2010b).

Additionally the high selectivity in detecting H₂S and its complete aqueous solubility are considered appreciable points throughout the analytical community (Galardon et al. 2009).

The development of this device is appreciable because we have shown that it is possible to implement a biosensor using a commercial and cheap protein.

Chapter four - Materials and Methods

Extraction and purification proteins

Cytochrome c peroxidase is a soluble 34-kDa heme protein, located in the intermembrane space of yeast mitochondria expressed in *E. coli*. Ccp was prepared in University of Leiden (Holland) in the lab of the Prof. G.W. Canters, in according with literature procedures reported in (Worrall et al. 2001). Myoglobin from horse skeletal muscle was bought from Sigma Aldrich (M0630) and used without further purifications.

Protein labelling

CcP and Myoglobin were labelled at the N-terminus with NHS-reactive fluorophors in a roughly 10 times molar excess over the proteins concentration potassium phosphate 100mM, pH 6,8 using procedure reported in literature (Kuznetsova et al. 2006)(fig.32).

The constructs were purified using PD-10 gel-filtration columns purchased from Amersham Pharmacia Biotech. Labeling ratios were in the range of 0.2 - 0.9 (dye molecule/protein), as determined from the absorption spectra of the labeled

proteins using the extinction coefficients at 280nm (Yonetani et al. 1972) for the protein and at 620nm for the Atto620 label, at 645 nm for the Cy5 label and at 550 nm for the Cy3 label as stated by the manufacturers, respectively.

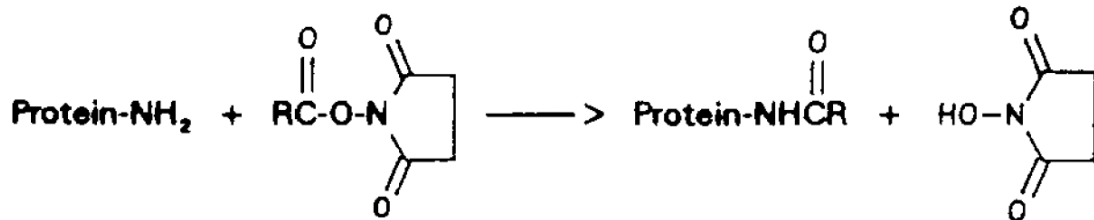


Fig. 32 Example of protein labeling reaction at the N-terminus with NHS-reactive fluorophors

Forster radius calculation

Values for the Förster radius, R_0 were calculated from the equation (Lakovicz J.R. 1996)

$$R_0 = 0.211(J\kappa^2n^{-4}FD)^{1/6} (\text{Å})$$

Here κ^2 is an orientation factor, n – refractive index, FD – fluorescence quantum yield of the donor and J – spectral overlap integral, defined as $J = \int FD(\lambda)eA(\lambda)\lambda^4d\lambda / \int FD(\lambda)d\lambda$, here $FD(\lambda)$ is the fluorescence intensity of the donor, $eA(\lambda)$ – the extinction coefficient in $[M^{-1} cm^{-1}]$ of the acceptor at wavelength λ with λ expressed in nanometers. The refractive index was taken as 1.4 and the orientation factor κ^2 was taken as 2/3 (Lakovicz J.R. 1996; Stryer and

Haugland 1967). FD for Cy5 was taken as 0.27 (Mujumdar et al. 1993), for Atto620 as 0.5 (as stated by the manufacturers). The distance (R) from the Cy5 and Atto620 labels to the active site was estimated as $R = [(d + 1) \pm 0.5]$ nm (adding 1 nm to the calculated distance d accounts for the approximate length of the linker chain), where d is the distance from the attachment point of the dye (N-terminus) to the Fe atom in the heme. The distance d was estimated as 3.0 nm from the crystal structure of CcP from baker's yeast [1ZBY].

Absorption and fluorescence measurements

Absorption spectra were recorded on a Cary-50 Spectrophotometer. For the solution measurements fluorescence spectra and time traces were measured on a Cary Eclipse Spectrophotometer. For the sol-gel measurements fluorescence spectra and time traces were also measured on a Cary Eclipse Spectrophotometer by fixing the quartz slides with a home made device in a 10×10 mm² airtight quartz fluorescence cuvette (Hellma Benelux bv, Rijswijk, Netherlands) and applying front face illumination (Lakovicz J.R. 1996) Measurements were performed in potassium phosphate buffer (100 mM, pH 6.8) at room temperature. High quality argon (< 1 ppm O²) was used to deoxygenate the sample prior to each measurement and to displace NO and H₂S, buffer and every all used component. For NO titrations, the cuvette was filled with deoxygenated sample solutions, after which μL amounts of an NO saturated buffer were injected.

Release NO product and NO saturated solution

Mahma Nonoate (Sigma Aldrich) are compound reliable generation of nitric oxide *in vitro* and *in vivo* and have with half-life time for NO release at 22 – 25°C of 3 min (Larry K.Keefe et al. 1996). NONOates or 1-substituted diazen-1-ium-1,2-diolates are compounds containing the $[N(O)NO]^-$ functional group that have proved useful for the reliable generation of nitric oxide (NO) *in vitro* and *in vivo* (Larry K.Keefe et al. 1996)(fig.32).

Saturated solutions of nitrogen monoxide were prepared by bubbling NO gas, produced *in situ* according to literature procedures (B.Mattson 2003) through 5mL of 100mM potassium phosphate (pH 6,8) for periods of up to 1 h resulting in an approximate concentration of 2mM at 20°C. (G.W.C.Kaye 1966).

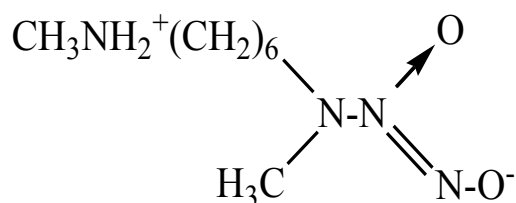


Fig. 33 Mahma NONOate. Systematic name (Z)-1-{N-Methyl-N-[6-(N-methylammoniohexy)amino]}diazene-1-ium-1,2diolate

H₂S and (NH₄)₂S saturated solutions o synthesis

Saturated solutions of H₂S were prepared by bubbling H₂S gas, produced *in situ* according to literature procedures (B.Mattson 2003), through 5 ml of 100 mM potassium phosphate (pH 6.8) for periods of up to 1h resulting in an approximate concentration of 12 mM at 20°C (G.W.C.Kaye 1966). Standard solutions of (NH₄)₂S were prepared by a 40% (v/v) commercial solution of (NH₄)₂S. The H₂S content of each solution was assessed by an independent coulombometric titration experiment.

Sol Gel matrix

The preparation of silica gels and the encapsulation of proteins were undertaken with pure TMOS (Zauner et al. 2008). TMOS (15.22 g) was mixed with milliQ water (3.38g) in a 1:2 molar ratio followed by the addition of 20 ml of 10mM HCl. The reaction mixture was sonicated for 20 minutes. Upon addition of buffer (potassium phosphate 100 mM, pH 6.8) in a 1:1 (volume) ratio and addition of roughly 1 ml of labeled protein solution (end conc. of protein: 5-10 MM) the mixture was degassed by bubbling through pure argon. Before gelation 150mL of the sol solution was quickly poured onto a home made device (8x30 mm² quartz slide Heraeus 3 quality with a 1 mm thickness) yielding a roughly 0.6mm thick sol-gel layer on top of the quartz slide. Activation of quartz slides with “Piranha solution” (30% H₂O₂ and concentrated H₂SO₄ in a 1:3 volume ratio) was

performed before pouring the sol solution on top. [Caution: “Piranha solution” is highly corrosive and should be handled with extreme care]. Samples were kept sealed with parafilm and allowed to age at 4°C overnight before use. Methanol, a by-product of the TMOS-based sol-gel process, was removed by washing the samples with potassium phosphate buffer (100 mM, pH 6.8) several times.

Cells cultures and treatments

Cell suspension culture were generated from hypocotyls dissected from young plants of *Arabidopsis* (*Arabidopsis thaliana* ecotype Landsberg erecta) and subcultured in AT3 medium (Radhika Desikan et al. 1996). For the subculture cycles, 10 mL of packed cell volume was placed in 250-mL Erlenmeyer flasks containing 50 mL of liquid medium. The cells were subcultured in a fresh medium at 7-d intervals and maintained in a phytotron on a horizontal rotary shaker (110 rpm) at 24°C ±1°C with a 8-h photoperiod and a light intensity of 60 $\mu\text{mol m}^{-2} \text{s}^{-1}$. Treatments with filter-sterilized solutions of CdCl_2 , were carried out with 3-d-old cultures.

Suspension cell cultures and heavy metal stress in close system

Suspension cell cultures were prepared in closed vials and then stressed with CdCl₂ 10mM solution (Carlo Erba) using a 100µl Hamilton gastight syringe. Before each experiment high quality argon (< 1 ppm O₂) was used to deoxygenate the vials as well as the other components. All the solutions were deoxygenated before use. The cells were sampled with a 1 mL Hamilton syringe gastight.

Internal Cd²⁺ Quantification

The Arabidopsis cells were collected by centrifugation of 2mL of suspension culture at 1,000g for 3 min. External Cd²⁺ was removed by washing the pelleted cells twice with 10mL of deionized water, two times with 10mL of 10mM EDTA, and finally two more times with 10mL of deionized water. After each wash, the cells were recollected by centrifugation and the supernatant was discarded in order to avoid cross contamination with extracellular Cd²⁺ contained in the liquid medium. Cells were then dried for 24 h at 60°C and accurately weighed. Internal Cd²⁺ was released by incubation with 5 mL of 0.1 M HCl for 40 min at 50°C. The metal content of the different samples was estimated using an atomic spectrometer (AAAnalyst 100, Perkin Elmer), and the concentration values were obtained using a calibration curve and normalizing for the dry weight.

H₂S measured and NO Quantification by fluorescence Analysis

Extracellular NO was determined by fluorimetric assay through its binding to the specific fluorophore DAF-2 (Sigma Aldrich) (Nakatsubo et al. 1998) and through an optical biosensor Ccp_Atto620. The calibration curve was created using ad-hoc standards prepared with Mahma NOnoate (Sigma Aldrich), a compound stored at – 20°C that releases NO in few seconds.

NO was quantified as the fold number compared with the untreated cells (relative fluorescence). All the reactions were carried out at least in duplicate, and their reproducibility was checked.

H₂S was determined through Mb_Atto620 optical biosensor. All the measurements of the fluorescence were carried out with a Cary Eclipse Spectrophotometer (Varian, Palo Alto USA).

References

- Arnaud, N., Murgia, I., Boucherez, J., Briat, J. F., Cellier, F., and Gaymard, F. (2006). An iron-induced nitric oxide burst precedes ubiquitin-dependent protein degradation for Arabidopsis AtFer1 ferritin gene expression. *Journal of Biological Chemistry* **281**, 23579-23588.
- B.Mattson, M. A. S. M. (2003). Microscale Gas Chemistry Book Educational Innovations . *Microscale Gas Chemistry Book Educational Innovations*.
- Ball, J. C., Hurley, M. D., Straccia, A. M., and Gierczak, C. A. (1999). Thermal release of nitric oxide from ambient air and diesel particles. *Environmental Science & Technology* **33**, 1175-1178.
- Barker, S. L., Clark, H. A., Swallen, S. F., Kopelman, R., Tsang, A. W., and Swanson, J. A. (1999a). Ratiometric and fluorescence-lifetime-based biosensors incorporating cytochrome c' and the detection of extra- and intracellular macrophage nitric oxide
14. *Anal.Chem.* **71**, 1767-1772.
- Barker, S. L. and Kopelman, R. (1998). Development and cellular applications of fiber optic nitric oxide sensors based on a gold-adsorbed fluorophore. *Anal.Chem.* **70**, 4902-4906.
- Barker, S. L., Kopelman, R., Meyer, T. E., and Cusanovich, M. A. (1998). Fiber-optic nitric oxide-selective biosensors and nanosensors. *Anal.Chem.* **70**, 971-976.
- Barker, S. L., Zhao, Y., Marletta, M. A., and Kopelman, R. (1999b). Cellular applications of a sensitive and selective fiber-optic nitric oxide biosensor based on a dye-labeled heme domain of soluble guanylate cyclase
31. *Anal.Chem.* **71**, 2071-2075.

- Bates, J. N., Baker, M. T., Guerra, R., and Harrison, D. G. (1991). Nitric-Oxide Generation from Nitroprusside by Vascular Tissue - Evidence That Reduction of the Nitroprusside Anion and Cyanide Loss Are Required. *Biochemical Pharmacology* **42**, S157-S165.
- Beligni, M. V., Fath, A., Bethke, P. C., Lamattina, L., and Jones, R. L. (2002). Nitric oxide acts as an antioxidant and delays programmed cell death in barley aleurone layers. *Plant Physiology* **129**, 1642-1650.
- Beligni, M. V. and Lamattina, L. (2000). Nitric oxide stimulates seed germination and de-etiolation, and inhibits hypocotyl elongation, three light-inducible responses in plants. *Planta* **210**, 215-221.
- Berney C. and Danuser G. (2003). FRET or No FRET: A Quantitative Comparison. *Biophysical Journal* **84**, 3992-4010.
- Berzofsky Jay A., Peisach J., and Blumberg W.E. (1971). Sulfheme proreins. I. Optical and magnetic properties of sulfmyoglobin and its derivateves. *Journal of Biological Chemistry* **246**, 3367-3377.
- Berzofsky Jay A., Peisach J., and Horecker B.L (1972). Sulfheme Proteins IV. The Stoichiometry of sulfur incorporation and the isolation of sulfhemin, the prostetic group of sulfmyoglobin. *The journal of biological chemistry* **247**, 3783-3791.
- Besson-Bard, A., Gravot, A., Richaud, P., Auroy, P., Duc, C., Gaymard, F., Tacconnat, L., Renou, J. P., Pugin, A., and Wendehenne, D. (2009). Nitric Oxide Contributes to Cadmium Toxicity in Arabidopsis by Promoting Cadmium Accumulation in Roots and by Up-Regulating Genes Related to Iron Uptake. *Plant Physiology* **149**, 1302-1315.
- Besson-Bard, A., Pugin, A., and Wendehenne, D. (2008). New insights into nitric oxide signaling in plants. *Annual Review of Plant Biology* **59**, 21-39.
- Boon, E. M. and Marletta, M. A. (2006). Sensitive and selective detection of nitric oxide using an H-NOX domain. *Journal of the American Chemical Society* **128**, 10022-10023.
- Borisov, S. M. and Wolfbeis, O. S. (2008). Optical biosensors. *Chemical Reviews* **108**, 423-461.
- Bowen, O. T., Erf, G. F., Chapman, M. E., and Wideman, R. F. (2007). Plasma nitric oxide concentrations in broilers after intravenous infections of lipopolysaccharide or microparticles. *Poultry Science* **86**, 2550-2554.

- Carimi, F., Zottini, M., Costa, A., Cattelan, I., De Michele, R., Terzi, M., and Lo Schiavo, F. (2005). NO signalling in cytokinin-induced programmed cell death. *Plant Cell and Environment* **28**, 1171-1178.
- Chan M.K.J. (2000). *Porphyryns Phthalocyanines* **4**, 358.
- Chan M.K.J. (2001). *Cur Opin Chem Biol* **5**, 216.
- Chapman, M. E. and Wideman, R. F. (2006). Evaluation of total plasma nitric oxide concentrations in broilers infused intravenously with sodium nitrite, lipopolysaccharide, aminoguanidine, and sodium nitroprusside. *Poultry Science* **85**, 312-320.
- Chen C.Q., Xin H., and Zhu Y.Z. (2007). Hydrogen sulphide: third gaseous transmitter, but with great phamacological potential. *Acta Pharmacol.Sin* **28**, 1709-1716.
- Choi M.M.F. and Hawkins P. (1997). Development of sulphide-selective optode membranes based on fluorescence quenching. *Anal Chim Acta* **344**, 105-110.
- Choi M.M.F. and Hawkins P. (2003). Development of an optical hydrogen sulphide sensor. *Sens.Actuators* **90**, 211-215.
- Clegg R (1996). 'Fluorescence resonance energy transfer.In Fluorescence Imaging Spectroscopy and Microscopy.'
- Clemens, S. (2006). Toxic metal accumulation, responses to exposure and mechanisms of tolerance in plants. *Biochimie* **88**, 1707-1719.
- De Michele, R., Vurro, E., Rigo, C., Costa, A., Elviri, L., Di Valentin, M., Careri, M., Zottini, M., di Toppi, L. S., and Lo Schiavo, F. (2009). Nitric Oxide Is Involved in Cadmium-Induced Programmed Cell Death in Arabidopsis Suspension Cultures. *Plant Physiology* **150**, 217-228.
- de Pinto, M. C., Paradiso, A., Leonetti, P., and De Gara, L. (2006). Hydrogen peroxide, nitric oxide and cytosolic ascorbate peroxidase at the crossroad between defence and cell death. *Plant Journal* **48**, 784-795.
- Delledonne, M. (2005). NO news is good news for plants. *Current Opinion in Plant Biology* **8**, 390-396.
- Delledonne, M., Zeier, J., Marocco, A., and Lamb, C. (2001). Signal interactions between nitric oxide and reactive oxygen intermediates in

- the plant hypersensitive disease resistance response. *Proceedings of the National Academy of Sciences of the United States of America* **98**, 13454-13459.
- di Toppi, L. S. and Gabbrielli, R. (1999). Response to cadmium in higher plants. *Environmental and Experimental Botany* **41**, 105-130.
- Doeller J.E. et al (2005). Polarographic measurement of hydrogen sulfide production and consumption by mammalian tissues. *Anal. Biochem.* **341**, 40-51.
- Dooly, G., Fitzpatrick, C., and Lewis, E. (2008). Optical sensing of hazardous exhaust emissions using a UV based extrinsic sensor. *Energy* **33**, 657-666.
- Durner, J. and Klessig, D. F. (1999). Nitric oxide as a signal in plants. *Current Opinion in Plant Biology* **2**, 369-374.
- E. Culotta, D. E. K. Jr. (1992). The Molecule of the Year. *Science* **258**, 1862-1865.
- E. Hawe, G. Dooly, C. Fitzpatrick, P. Chambers, E. Lewis, W. Z. Zhao, T. Sun, K. T. V. Grattan, M. Degner, H. Ewald, S. Lochmann, G. Bramman, C. Wei, D. Hitchen, J. Lucas, A. Al-Shamma'a, E. Merlone-Borla, P. Faraldi, M. Pidria, (2007). Measuring of exhaust gas emissions using absorption spectroscopy. *Int. J. Intell. Syst. Technol. Appl* **3**, 33-51.
- Ebelmen M. (1847). 'Sur l'hyalite artificielle et l'hydrophane, Comptes Rendus de l'Académie des Sciences de Paris.'
- Edwards, S. L. and Poulos, T. L. (1990). Ligand-Binding and Structural Perturbations in Cytochrome-C Peroxidase - A Crystallographic Study. *Journal of Biological Chemistry* **265**, 2588-2595.
- Forster T. (1948). Intermolecular energy migration and fluorescence. *Ann. Phys* **2**, 55-75.
- Franz, K. J., Singh, N., Spingler, B., and Lippard, S. J. (2000). Aminotroponimines as ligands for potential metal-based nitric oxide sensors
12. *Inorg. Chem.* **39**, 4081-4092.
- Fuller D.C. and Suruda J. (2000). Occupationally related hydrogen sulfide deaths in the United States from 1984 - 1994. *J. Occup. Environ. Med.* **42**, 939-942.

- G.Dooly, C. Fitzpatrick, E. Lewis, (2007). Hazardous exhaust gas monitoring using a deep UV based differential optical absorption spectroscopy (DOAS) system. *J.Phys.Conf.Ser* 76.
- G.W.C.Kaye, T. H. L. (1966). Tables of Physical and Chemical Constants. Longmans, London.
- Galardon, E., Tomas, A., Roussel, P., and Artaud, I. (2009). New fluorescent zinc complexes: towards specific sensors for hydrogen sulfide in solution. *Dalton Transactions* 9126-9130.
- Garces, H., Durzan, D., and Pedroso, M. C. (2001). Mechanical stress elicits nitric oxide formation and DNA fragmentation in *Arabidopsis thaliana*. *Annals of Botany* 87, 567-574.
- Gould, K. S., Lamotte, O., Klinguer, A., Pugin, A., and Wendehenne, D. (2003). Nitric oxide production in tobacco leaf cells: a generalized stress response? *Plant Cell and Environment* 26, 1851-1862.
- Gruber, H. J., Hahn, C. D., Kada, G., Riener, C. K., Harms, G. S., Ahrer, W., Dax, T. G., and Knaus, H. G. (2000). Anomalous fluorescence enhancement of Cy3 and Cy3.5 versus anomalous fluorescence loss of Cy5 and Cy7 upon covalent linking to IgG and noncovalent binding to avidin. *Bioconjugate Chemistry* 11, 696-704.
- Hirsch, A. R. (2002). Hydrogen sulfide exposure without loss of consciousness: chronic effects in four cases. *Toxicology and Industrial Health* 18, 51-61.
- Horemans, N., Raeymaekers, T., Van Beek, K., Nowocin, A., Blust, R., Broos, K., Cuypers, A., Vangronsveld, J., and Guisez, Y. (2007). Dehydroascorbate uptake is impaired in the early response of *Arabidopsis* plant cell cultures to cadmium. *Journal of Experimental Botany* 58, 4307-4317.
- J.A.Kramer (1992). Hydrogen Sulfide detectors and determination. *Turbomachinery* 30-32.
- Jorgensen C.K. (1962). Absorption Spectra and chemical bonding in complexes 61. (Ed. P. O. Pergamon.)
- Kellin D. (1925). *Proc.R.Soc.London* 98, 312.
- Kennedy M.L and Gibney B.R. (2001). Metalloprotein and redox protein design. *Structural Biology* 11, 485-490.

- Kikuchi, K., Nagano, T., Hayakawa, H., Hirata, Y., and Hirobe, M. (1993). Real time measurement of nitric oxide produced ex vivo by luminol-H₂O₂ chemiluminescence method
6. *J.Biol.Chem.* **268**, 23106-23110.
- Kojima, H., Nakatsubo, N., Kikuchi, K., Kawahara, S., Kirino, Y., Nagoshi, H., Hirata, Y., and Nagano, T. (1998). Detection and imaging of nitric oxide with novel fluorescent indicators: Diaminofluoresceins
39. *Analytical Chemistry* **70**, 2446-2453.
- Kopyra, M. and Gwozdz, E. A. (2003). Nitric oxide stimulates seed germination and counteracts the inhibitory effect of heavy metals and salinity on root growth of *Lupinus luteus*. *Plant Physiology and Biochemistry* **41**, 1011-1017.
- Kopyra, M., Stachon-Wilk, M., and Gwozdz, E. A. (2006). Effects of exogenous nitric oxide on the antioxidant capacity of cadmium-treated soybean cell suspension. *Acta Physiologiae Plantarum* **28**, 525-536.
- Koshland, D. E., Jr. (1992). The molecule of the year
Science **258**, 1861.
- Kotake, Y., Tanigawa, T., Tanigawa, M., Ueno, I., Allen, D. R., and Lai, C. S. (1996). Continuous monitoring of cellular nitric oxide generation by spin trapping with an iron-dithiocarbamate complex
Biochim.Biophys.Acta **1289**, 362-368.
- Kuznetsova, S., Zauner, G., Schmauder, R., Mayboroda, O. A., Deelder, A. M., Aartsma, T. J., and Canters, G. W. (2006). A Forster-resonance-energy transfer-based method for fluorescence detection of the protein redox state
Anal.Biochem. **350**, 52-60.
- Lakovicz J.R. (1996). 'Principles of Fluorescence Spectroscopy.' (Kluwer Academic/Plenum, New York, Boston, Dordrecht, Moscow:
- Lakovicz J.R. (1999). Energy transfer. In Principles of fluorescence Spectroscopy. pp. 367-94.
- Lamattina, L., Garcia-Mata, C., Graziano, M., and Pagnussat, G. (2003). Nitric oxide: The versatility of an extensive signal molecule. *Annual Review of Plant Biology* **54**, 109-136.

- Larry K.Keefer, raymond W.Nims, Keith M.Davies, and David A.Wink (1996). "NONOates" (1-substituted diazen-1-ium1,2-diolates) as Nitric Oxide Donors: Convenient Nitric Oxide Dosage Forms. *Methods in Enzymology* **268**, 281-293.
- Leshem, Y. Y. and Haramaty, E. (1996). The characterization and contrasting effects of the nitric oxide free radical in vegetative stress and senescence of *Pisum sativum* Linn foliage. *Journal of Plant Physiology* **148**, 258-263.
- Li L. and Moore P.K. (2007). An a overview of biological significance of endogeneous gases: new rules of old molecules. *Biochem Soc.Trans* **35**, 1138-1141.
- Li L. and Moore P.K. (2008). Putative biological rules of hydrogen sulphide in health and disease: a breath of not so fresh air? *Trends Pharmacol Science* **29**, 84-90.
- Lim, M. H. and Lippard, S. J. (2004). Fluorescence-based nitric oxide detection by ruthenium porphyrin fluorophore complexes. *Inorganic Chemistry* **43**, 6366-6370.
- Lim, M. H. and Lippard, S. J. (2007). Metal-based turn-on fluorescent probes for sensing nitric oxide
Acc.Chem.Res. **40**, 41-51.
- Mao, L., Shi, G., Tian, Y., Liu, H., Jin, L., Yamamoto, K., Tao, S., and Jin, J. (1998). A novel thin-layer amperometric detector based on chemically modified ring-disc electrode and its application for simultaneous measurements of nitric oxide and nitrite in rat brain combined with in vivo microdialysis
Talanta **46**, 1547-1556.
- Martin, A. C., Orengo, C. A., Hutchinson, E. G., Jones, S., Karmirantzou, M., Laskowski, R. A., Mitchell, J. B., Taroni, C., and Thornton, J. M. (1998). Protein folds and functions. *Structure* **6**, 875-884.
- McMunn C.A. (1886). *J.Phystol* **5**.
- Miller, M. A., Shaw, A., and Kraut, J. (1994). 2.2 A structure of oxy-peroxidase as a model for the transient enzyme: peroxide complex
Nat.Struct.Biol. **1**, 524-531.

- Mujumdar, R. B., Ernst, L. A., Mujumdar, S. R., Lewis, C. J., and Waggoner, A. S. (1993). Cyanine dye labeling reagents: sulfoindocyanine succinimidyl esters
Bioconjug.Chem. **4**, 105-111.
- Murgia, I., Delledonne, M., and Soave, C. (2002). Nitric oxide mediates iron-induced ferritin accumulation in Arabidopsis. *Plant Journal* **30**, 521-528.
- Nagano, T. and Yoshimura, T. (2002). Bioimaging of nitric oxide
Chem.Rev. **102**, 1235-1270.
- Nakatsubo, N., Kojima, H., Kikuchi, K., Nagoshi, H., Hirata, Y., Maeda, D., Imai, Y., Irimura, T., and Nagano, T. (1998). Direct evidence of nitric oxide production from bovine aortic endothelial cells using new fluorescence indicators: diaminofluoresceins. *FEBS Letters* **427**, 263-266.
- Neill, S. J., Desikan, R., and Hancock, J. T. (2003). Nitric oxide signalling in plants. *New Phytologist* **159**, 11-35.
- Nicholls P. (1961). The formation and properties of Sulphmyoglobin and Sulphcatalase. *Biochemistry J.* 374-383.
- Nishimura, H., Hayamizu, T., and Yanagisawa, Y. (1986). Reduction of No₂ to No by Rush and Other Plants. *Environmental Science & Technology* **20**, 413-416.
- Noriega, G. O., Yannarelli, G. G., Balestrasse, K. B., Batlle, A., and Tomaro, M. L. (2007). The effect of nitric oxide on heme oxygenase gene expression in soybean leaves. *Planta* **226**, 1155-1163.
- P.K.Lala (1998). Significance of nitric oxide in carcinogenesis, tumor progression and cancer therapy. *Cancer Metastasis Rev* **17**, 1-6.
- Paoli M., Marles-Wright J, and Smith A. (2002). *DNA Cell Biol* **21**, 271.
- Pierre A.C. (2004). 'Biocatalysis and Biotransformation.'
- Piqueras, A., Olmos, E., Martinez-Solano, J. R., and Hellin, E. (1999). Cd-induced oxidative burst in tobacco BY2 cells: Time course, subcellular location and antioxidant response. *Free Radical Research* **31**, S33-S38.
- Pond, A. E., Sono, M., Elenkova, E. A., McRee, D. E., Goodin, D. B., English, A. M., and Dawson, J. H. (1999). Magnetic circular dichroism studies of

the active site heme coordination sphere of exogenous ligand-free ferric cytochrome c peroxidase from yeast: effects of sample history and pH
J.Inorg.Biochem. **76**, 165-174.

Radhika Desikan, John T.Hancock, Marcus J.Coffey, and Steven J.Neill (1996). Generation of active oxygen in elicited cells of *Arabidopsis thaliana* is mediated by a NADPH oxidase-like enzyme. *FEBS Letters* 213-217.

Reiffestein R.G. and Hulbert W.C. (1992). Toxicology of Hydrogen Sulphide. *Ann Rev Pharmacol Toxicol* **32**, 109-134.

Rodriguez-Fernandez J, Costa M.J., Pereiro R., and Sanz Mendel A. (1999). Simple detector for oral malodour based on spectrofluorimetric measurements of hydrogen sulphide in mouth air. *Anal Chim Acta* **398**, 31.

Rodriguez-Serrano, M., Romero-Puertas, M. C., Zabalza, A., Corpas, F. J., Gomez, M., Del Rio, L. A., and Sandalio, L. M. (2006). Cadmium effect on oxidative metabolism of pea (*Pisum sativum* L.) roots. Imaging of reactive oxygen species and nitric oxide accumulation in vivo. *Plant Cell and Environment* **29**, 1532-1544.

Roncaroli, F., Olabe, J. A., and van Eldik, R. (2003). Kinetics and mechanism of the interaction of nitric oxide with pentacyanoferrate(II). Formation and dissociation of $[\text{Fe}(\text{CN})_5\text{NO}](3-)$. *Inorganic Chemistry* **42**, 4179-4189.

Sato, M., Hida, N., and Umezawa, Y. (2005). Imaging the nanomolar range of nitric oxide with an amplifier-coupled fluorescent indicator in living cells *Proc.Natl.Acad.Sci.U.S.A* **102**, 14515-14520.

Schmidt, H. H. H. W. and Walter, U. (1994). NO at Work. *Cell* **78**, 919-925.

Sellers, V. M., Wu, C. K., Dailey, T. A., and Dailey, H. A. (2001). Human ferrochelatase: Characterization of substrate-iron binding and proton-abstracting residues
Biochemistry **40**, 9821-9827.

Spiro T.G. and Jarzecki A.A. (2001). Heme-based sensor: theoretical modeling of heme-ligand-protein interaction. *Chemical Biology* **5**, 715-723.

Stamler, J. S. (1994). Redox Signaling - Nitrosylation and Related Target Interactions of Nitric-Oxide. *Cell* **78**, 931-936.

Stamler, J. S., Singel, D. J., and Loscalzo, J. (1992). Biochemistry of Nitric-Oxide and Its Redox-Activated Forms. *Science* **258**, 1898-1902.

- Strianese, M., De Martino, F., Pavone, V., Lombardi, A., Canters, G. W., and Pellecchia, C. (2010a). A FRET-based biosensor for NO detection. *Journal of Inorganic Biochemistry* **104**, 619-624.
- Strianese, M., De Martino, F., Pellecchia, C., Ruggiero, G., and D'Auria, S. (2010b). Myoglobin As A New Fluorescence Probe to Sense H(2)S. *Protein Pept.Lett.*
- Stryer, L. (1978). Fluorescence energy transfer as a spectroscopic ruler. *Annu.Rev.Biochem* **47**, 819-846.
- Stryer, L. and Haugland, R. P. (1967). Energy transfer: a spectroscopic ruler *Proc.Natl.Acad.Sci.U.S.A* **58**, 719-726.
- Thomsen, L. L. and Miles, D. W. (1998). Role of nitric oxide in tumour progression: Lessons from human tumours *Cancer and Metastasis Reviews* **17**, 107-118.
- Tsushida R (1938). Absorption spectra of coordination compounds *Bull.Soc.Japan* 388-400.
- White, B. R., Liljestrand, H. M., and Holcombe, J. A. (2008). A 'turn-on' FRET peptide sensor based on the mercury binding protein MerP *Analyst* **133**, 65-70.
- Wildt, J., Kley, D., Rockel, A., Rockel, P., and Segschneider, H. J. (1997). Emission of NO from several higher plant species. *Journal of Geophysical Research-Atmospheres* **102**, 5919-5927.
- Wilson, I. D., Neill, S. J., and Hancock, J. T. (2008). Nitric oxide synthesis and signalling in plants. *Plant Cell and Environment* **31**, 622-631.
- Wink, D. A. and Mitchell, J. B. (1998). Chemical biology of nitric oxide: Insights into regulatory, cytotoxic, and cytoprotective mechanisms of nitric oxide. *Free Radical Biology and Medicine* **25**, 434-456.
- Worrall, J. A. R., Kolczak, U., Canters, G. W., and Ubbink, M. (2001). Interaction of yeast iso-1-cytochrome c with cytochrome c peroxidase investigated by [N-15,H-1] heteronuclear NMR spectroscopy. *Biochemistry* **40**, 7069-7076.
- Wu X.C., Samminaiken R., and Zhang W.J. (2007). Measurement of low concentration and nano-quantity hydrogen sulfide in aqueous solution: measurement mechanisms and limitations. *Meas Sci Technol* **18**, 1315-1320.

- Wu, C. K., Dailey, H. A., Rose, J. P., Burden, A., Sellers, V. M., and Wang, B. C. (2001). *Nat.Struct.Biol.* **8**, 156.
- Yamasaki, H. (2000). Nitrite-dependent nitric oxide production pathway: implications for involvement of active nitrogen species in photoinhibition in vivo. *Philosophical Transactions of the Royal Society B-Biological Sciences* **355**, 1477-1488.
- Yonetani, T. and Anni, H. (1987). Yeast cytochrome c peroxidase. Coordination and spin states of heme prosthetic group. *J.Biol.Chem.* **262**, 9547-9554.
- Yonetani, T., Yamamoto, H., Erman, J. E., Leigh, J. S., Jr., and Reed, G. H. (1972). Electromagnetic properties of hemoproteins. V. Optical and electron paramagnetic resonance characteristics of nitric oxide derivatives of metalloporphyrin-apohemoprotein complexes. *J.Biol.Chem.* **247**, 2447-2455.
- Zauner, G., Lonardi, E., Bubacco, L., Aartsma, T. J., Canters, G. W., and Tepper, A. W. (2007). Tryptophan-to-dye fluorescence energy transfer applied to oxygen sensing by using type-3 copper proteins. *Chemistry* **13**, 7085-7090.
- Zauner, G., Strianese, M., Bubacco, L., Aartsma, T. J., Tepper, A. W. J. W., and Canters, G. W. (2008). Type-3 copper proteins as biocompatible and reusable oxygen sensors. *Inorganica Chimica Acta* **361**, 1116-1121.

Acknowledgements

I express my profound gratitude and deep appreciation to Prof. C.Pellecchia for accepting me as a member of Bioinorganic group and his guidance during this work

I am most grateful to Dr. Mariella Strianese for support, confidence and fruitful discussion of my work

My profound gratitude goes to Prof. G. Canters for his fruitful discussion of this work

I am also grateful to Prof. S. Castiglione and Dr. A. Cicatelli for the contribution, correction of this manuscript and technical assistance during the period of this work

I sincerely thank the staffs of work group and the Department of Chemistry for their friendly collaboration and assistance

Finally, I am indebted to my wife for her morale assistance and patience